The Pennsylvania State University

The Graduate School

College of Engineering

TITLE OF YOUR THESIS

A Dissertation

in Civil Engineering

by

Charilaos Lyritsakis

Submitted in Partial Fullfillment
of the Requirements
for the Degree of

Doctor of Philosophy

December 2022

The dissertation of Charilaos Lyritsakis was reviewed and approved* by the following:

Kostas Papakonstantinou
Associate Professor of Civil & Environmental Engineering
Dissertation Advisor
Chair of Committee

Gordon Warn
Associate Professor of Civil & Environmental Engineering

Pinlei Chen
Assistant Professor of Civil & Environmental Engineering

Tong Qiu
Professor of Civil & Environmental Engineering

Reuben Kraft
Associate Professor of Mechanical Engineering

Patrick Fox
Professor of Civil & Environmental Engineering
Head of Department of Civil & Environmental Engineering

* Signatures are on file in the Graduate School.

Abstract

Lorem ipsum dolor sit amet, consectetur adipiscing elit, sed do eiusmod tempor incididunt ut labore et dolore magna aliqua. Ut enim ad minim veniam, quis nostrud exercitation ullamco laboris nisi ut aliquip ex ea commodo consequat. Duis aute irure dolor in reprehenderit in voluptate velit esse cillum dolore eu fugiat nulla pariatur. Excepteur sint occaecat cupidatat non proident, sunt in culpa qui officia deserunt mollit anim id est laborum.

To my parents

Table of Contents

List of Figures viii

List of Tables ix

Nomenclature x

Acronyms xiii

Acknowledgements xiv

Chapter 1: Introduction and Background 1

Chapter 2: Hybrid Beam Element Formulation 2

2.1 Introduction 2

2.2 Geometrically-Exact Model 3

2.2.1 Beam Kinematics 3

2.2.2 Strain Measures, Strain-Displacement Relations 5

2.3 Nonlinear Programming Formulation 7

2.3.1 NLP framework 7

2.3.2 Total potential energy 8

2.3.3 Strain-Displacement Constraints 9

2.3.4 Lagrangian function 12
2.4 Implementation 12
2.4.1 Equilibrium 14
2.4.2 Hessian matrix 15
2.4.3 Solution scheme 15
2.4.4 Cross-section state determination 20
Chapter 3: Material Constitutive Model 25
3.1 Introduction 25
3.1.1 Notation 26
3.2 Three-dimensional Constitutive Model 26
3.3 The J_2 formulation for fiber stress state 28
3.3.1 Mapping on the constrained stress space 28
3.3.2 Continuous tangent modulus 32
3.4 Implicit integration of rate equations 32
3.4.1 Elastic predictor - Plastic Corrector algorithm 33
3.4.2 Consistent Tangent Modulus 35
3.4.3 Consistent Section Stiffness 36
Chapter 4: Discussion 38
Chapter 5: Conclusion 39
Appendix A: 41
A.0.1 Gradient of strain energy 41

A.0.2 Gradient of constraints 42

A.0.3 Gradient of the potential energy 45

A.0.4 Gradient of the Lagrangian 46

Appendix B: 47

Appendix C: 50

Appendix D: 52

References 53

List of Figures

2.1 Undeformed and deformed configurations of the beam. 4

2.2 Integration of curvature shape functions. 11

2.3 Typical element representing one member. 13

2.4 Solutions process stages. Quantities $\mathbf{K}^e$ and $\vec{\boldsymbol{F}}_{int}$ stand for stiffness matrix and internal nodal force vector for element e respectively. 24

3.1 Feasible space and yield locus for the J_2 model. At the boundary of the ellipse, $\sqrt{3J_2} = q$. 29

List of Tables

Nomenclature

$\vec{\boldsymbol{E}}_i$	Spatial basis unit vectors, $i = 1, 2, 3$
$\vec{\boldsymbol{e}}_i$	Material basis unit vectors, $i = 1, 2, 3$
X_i	Initial configuration coordinates, $i = 1, 2, 3$
$\vec{\boldsymbol{X}}$	Position vector of a material point in the initial configuration
x_i	Current configuration coordinates, $i = 1, 2, 3$
$\vec{\boldsymbol{x}}$	Position vector of a material point in the current configuration
$\vec{\boldsymbol{r}}_o$	Position vector of a material point on the centerline in the initial configuration
$\vec{\boldsymbol{r}}$	Position vector of a material point on the centerline in the current configuration
$\vec{\boldsymbol{u}}$	Displacement vector of points on the centerline with respect to the initial configuration.
$\vec{\boldsymbol{t}}$	Position vector of a material point on the local system of a cross-section.
ϕ	Angle between $\vec{\boldsymbol{E}}_i$ and $\vec{\boldsymbol{e}}_i$
$\mathbf{R}(\phi)$	Rotation matrix
κ	Curvature of the beam centerline.
ϵ	Axial strain of the beam centerline
γ	Shear strain of the beam centerline
$\vec{\boldsymbol{s}}$	Vector containing ϵ and γ but not κ
u	Displacement component along X_1
v	Displacement component along X_2
$\vec{\boldsymbol{d}}$	Displacement vector containing u, v and ϕ
$\vec{\boldsymbol{q}}$	Strain vector containing ϵ, γ and κ

f	Generic objective function
$\vec{\boldsymbol{h}}$	Vector of discretized constraints
$\mathcal{S}$	Constrained space for $\vec{\boldsymbol{x}}$
$\mathcal{L}$	Lagrangian function associated with the NLP
$\vec{\boldsymbol{\lambda}}$	Vector of Lagrange multipliers
Π	Total potential energy function
U	Strain energy function
W	Potential energy of external loads
$\mathcal{W}_s$	Cross-section strain energy density
$\vec{\boldsymbol{P}}$	Vector of external loads
$\vec{\boldsymbol{F}}_{sec}$	Cross-section stress resultants
N	Section axial force
V	Section shear force
M	Section internal moment
E	Young's modulus
G	Shear modulus
I	Cross-section moment of intertia
A	Cross-section area
A_s	Effective area of the cross-section
ℓ	Element length
n_{nod}	Number of non-restrained nodes
n	Number of quadrature points in the element
w_i	Quadrature weight for the i-th quadrature point
ξ	Normalized coordinate associated with X_1
L_i	Lagrange cardinal function
$\mathbf{T}$	Curvature mapping matrix
$\boldsymbol{\Theta}$	Vandermonde matrix

$\vec{\boldsymbol{y}}$	Internal field variable vector, associated with uknowns at quadrature points
$\boldsymbol{\Lambda}$	Element orientation matrix
θ	Angle of element centerline in the initial configuration with $\vec{\boldsymbol{E}}_1$
$\mathcal{E}^e$	Energy contribution of element e in the Lagrangian function
$\mathbf{H}$	Hessian matrix
$\vec{\boldsymbol{z}}$	Vector of all unknown state variables of the system
$\mathbf{k}_s$	Section stiffness matrix
$\mathbf{K}$	Stiffness matrix
$\vec{\boldsymbol{F}}_{int}$	Internal nodal force vector
ΔS	Incremental arc-length parameter
$\vec{\boldsymbol{\sigma}}_f$	Active stress components on a fiber
$\vec{\boldsymbol{\epsilon}}_f$	Strain components corresponding to $\vec{\boldsymbol{\sigma}}_f$
$\mathbf{N}_s$	Cross-section shape function matrix
φ	Shear strain distribution function along the cross-section height
$\mathbf{C}$	Material tangent modulus
$\vec{\boldsymbol{d}}_{lorr}$	Element nodal displacement vector for left (l) or right (r) elememtn edge
$\vec{\boldsymbol{P}}_{lorr}$	Element externally applied nodal force vector for left (l) or right (r) elememtn edge

Acronyms

DOF Degree of Freedom.

FEM Finite Element Method.

NLP Non-Linear Programming.

TPE Total Potential Energy.

Acknowledgements

Lorem ipsum dolor sit amet, consectetur adipiscing elit, sed do eiusmod tempor incididunt ut labore et dolore magna aliqua. Ut enim ad minim veniam, quis nostrud exercitation ullamco laboris nisi ut aliquip ex ea commodo consequat. Duis aute irure dolor in reprehenderit in voluptate velit esse cillum dolore eu fugiat nulla pariatur. Excepteur sint occaecat cupidatat non proident, sunt in culpa qui officia deserunt mollit anim id est laborum.

CHAPTER 1

INTRODUCTION AND BACKGROUND

CHAPTER 2

HYBRID BEAM ELEMENT FORMULATION

2.1 Introduction

In this chapter we present the formulation of a novel hybrid beam element which is based on NLP principles. The kinematic assumptions adopted fall under the category of geometrically exact or Simo-Reissner beam theory[1, 2, 3, 4], whereby no simplifying approximation is made with respect to the strain-displacement equations. This allows for capturing arbitrarily large displacements and rotations, as well as accounting for the effect of shear deformation at the section level.

As opposed to deriving the system equations from the Galerkin form,, we recast the problem in an NLP framework by utilizing the underlying variational structure. The total potential energy (TPE) functional is augmented with all relevant conditions that enforce the exact kinematics, by intoducing a set of Lagrange multipliers that act as conjugate force quantities. The resulting modified functional is then approximated by employing a Gauss-Legendre quadrature rule, which yields the objective function to be minimized. With this particular approach, the primary variables in the element interior contributing to the elastic strain energy are the generalized strain measures of the centroid, which are the unknown quantities at the quadrature points. Displacement measures at the edge nodes of the element, namely, the translations along coordinate axes and the rotation of cross sections, are only associated with the external work. Kinematic consistency between the rotational measures of displacement and strains is enforced by using a Lagrange interpolation scheme for the curvature field, similar to the one used by Neuenhofer and Filippou [5] and Schulz & Filippou [6] for force-based elements. In this work, the points used for the interpolation coincide with the integration points of the quadrature rule used for approximating the energy functional. To avoid ill-conditioning issues of the linearized operator, we also outline a block-elimination procedure for the linear system involving the Hessian matrix so that the reduced system includes only displacement components. The corresponding stiffness operator is well-conditioned, sparse, banded and symmetric. This renders standard FEM routines from existing codes reusable and, in conjuction with the capability for accuracy even with crude discretization, provides an attractive formulation for fast and accurate computation. Additionally, accuracy and locking free performance are guaranteed with just one element per structural member, even in the presence of arbitrarily large displacements and rotations. Accordingly, the element can also capture high curvature gradients due to plastic hinge formation, in the case of inelastic analysis.

This chapter starts with a brief outline of the beam geometric description while adhering to the derivations by Cardona & Geradin[7], follwed by the hybrid NLP formulation for the element. The chapter concludes with implementation details, where special attention is given to the block elimination technique used for the reduction of the linear system involving the Hessian matrix.

2.2 Geometrically-Exact Model

2.2.1 Beam Kinematics

Let $\{\mathbf{E}\}$ be a fixed orthonormal coordinate frame with unit vectors $\{\vec{\boldsymbol{E}}_1,\ \vec{\boldsymbol{E}}_2,\ \vec{\boldsymbol{E}}_3\}$ along the axes X_1, X_2, X_3. For an initially straight beam of length ℓ with its centerline coinciding with X_1, the undeformed configuration is completely described by:

$$\vec{\boldsymbol{X}}(X_1, X_2) = X_1\vec{\boldsymbol{E}}_1 + X_2\vec{\boldsymbol{E}}_2 = \vec{\boldsymbol{r}}_o(X_1) + \vec{\boldsymbol{t}}(X_2) \tag{2.1}$$

where $\vec{\boldsymbol{r}}_o$ traces the centerline in the reference configuration and $\vec{\boldsymbol{t}}$ locates a material point on the cross section. Assuming a rectangular cross-section of height h, without loss of generality, we have that $X_1 \in [0,\ \ell]$ and $X_2 \in [-h/2, h/2]$. We should note here that X_3 is

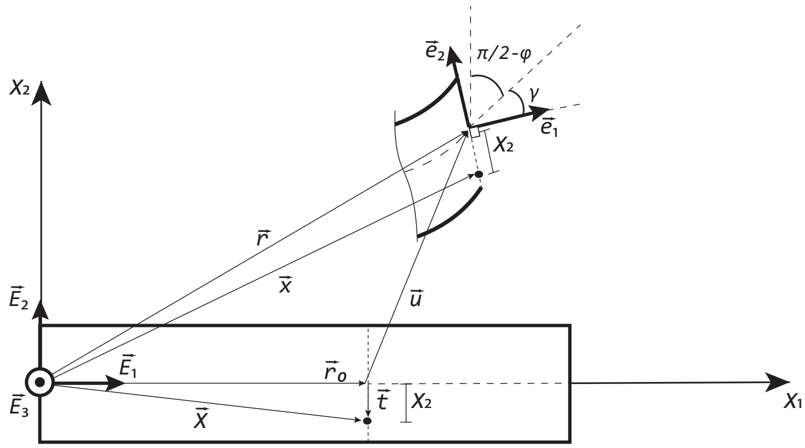

Fig. 2.1. Undeformed and deformed configurations of the beam.

omitted as it does not explicitly come into the expressions. We nevertheless hold on to the $\mathbb{R}^3$ vector formalism to maintain consistency with the representation of rotation as a linear operator. After the application of a displacement field $\vec{\boldsymbol{u}}(X_1)$, the deformed configuration is given by vector $\vec{\boldsymbol{x}}$ such that:

$$\vec{\boldsymbol{r}} = \vec{\boldsymbol{r}}_o + \vec{\boldsymbol{u}} \tag{2.2}$$

$$\vec{\boldsymbol{x}} = \vec{\boldsymbol{r}} + X_2 \vec{\boldsymbol{e}}_2 \tag{2.3}$$

where $\{\mathrm{e}\}$ is a local coordinate system attached at cross-sections that completely describes their orientation. For the unit vectors of the local base $\vec{\boldsymbol{e}}_1,\ \vec{\boldsymbol{e}}_2,\ \vec{\boldsymbol{e}}_3$, we let $\vec{\boldsymbol{e}}_1$ be normal to the cross-section, but not necessarily tangent to the deformed centerline, and $\vec{\boldsymbol{e}}_2$ (and $\vec{\boldsymbol{e}}_3$) coincide with the cross-section principal axes of inertia, as shown in Fig. (2.1).

If $\mathbf{R}$ is the rotation operator that rotates $\{\mathbf{E}\}$ to $\{\mathrm{e}\}$, then:

$$\vec{\boldsymbol{e}}_i = \mathbf{R}\vec{\boldsymbol{E}}_i, \quad i = 1, 2, 3 \tag{2.4}$$

For the plane case, the component form of $\mathbf{R}$ reduces to:

$$\mathbf{R} = \begin{bmatrix} \cos\phi & -\sin\phi & 0 \\ \sin\phi & \cos\phi & 0 \\ 0 & 0 & 1 \end{bmatrix} \tag{2.5}$$

Then, using Eq. (2.4), Eq. (2.3) becomes:

$$\vec{\boldsymbol{x}} = \vec{\boldsymbol{r}} + \mathbf{R}\vec{\boldsymbol{t}} \tag{2.6}$$

For Eqs. (2.3),(2.6) to hold in this manner, we tacitly assume that cross-sections remain rigid during deformation, that is, the position of a material point on a cross-section with respect to the centroid does not change.

2.2.2 Strain Measures, Strain-Displacement Relations

Within the context of geometrically-exact formulations, it is common to adopt as a strain measure $\vec{\boldsymbol{s}}$ the difference of the position vector gradients, $\vec{\boldsymbol{r}}$ and $\vec{\boldsymbol{r}}_o$, with respect to the local frame (e.g. see [2, 7, 8]). Denoting derivatives with respect to X_1 by $(\cdot)'$, we get:

$$\vec{\boldsymbol{s}} = \mathbf{R}^T\vec{\boldsymbol{r}}' - \vec{\boldsymbol{r}}_o' \tag{2.7}$$

whereas the cross-section curvature is given as:

$$\kappa = \phi' \tag{2.8}$$

The axial and shear strain of the centroid, ϵ and γ respectively, can then be retained as follows:

$$\epsilon = \vec{\boldsymbol{e}}_1^T \vec{\boldsymbol{s}} \tag{2.9}$$

$$\gamma = \vec{\boldsymbol{e}}_2^T \vec{\boldsymbol{s}} \tag{2.10}$$

where $\vec{\boldsymbol{s}} = \begin{bmatrix} \epsilon & \gamma & 0 \end{bmatrix}^T$, with the third component, representing the shear strain along the out-of-plane axis, being by assumption zero.

Using Eq. (2.2) and performing the differentiations in Eq. (2.7) with respect to X_1, we get:

$$\vec{\boldsymbol{s}} = \mathbf{R}^T[\vec{\boldsymbol{u}}' + \vec{\boldsymbol{E}}_1] - \vec{\boldsymbol{E}}_1 \tag{2.11}$$

Deriving the exact differential strain-displacement relations as presented in Reissner[1] is straigtforward if we solve Eq. (2.11) for $\vec{\boldsymbol{u}}'$:

$$\vec{\boldsymbol{u}}' = \mathbf{R}\vec{\boldsymbol{s}} + \vec{\boldsymbol{e}}_1 - \vec{\boldsymbol{E}}_1 \tag{2.12}$$

If we write $\vec{\boldsymbol{u}} = \begin{bmatrix} u & v & 0 \end{bmatrix}^T$, then the explicit expressions for u', v' along with Eq. (2.8) are:

$$u' = \vec{\boldsymbol{E}}_1^T \vec{\boldsymbol{u}}' = (1+\epsilon)\cos\phi - \gamma\sin\phi - 1 \tag{2.13a}$$

$$v' = \vec{\boldsymbol{E}}_2^T \vec{\boldsymbol{u}}' = (1+\epsilon)\sin\phi + \gamma\cos\phi \tag{2.13b}$$

$$\phi' = \kappa \tag{2.13c}$$

By introducing vectors $\vec{\boldsymbol{d}}$ and $\vec{\boldsymbol{q}}$, such that $\vec{\boldsymbol{d}} = \begin{bmatrix} u & v & \phi \end{bmatrix}^T$ and $\vec{\boldsymbol{q}} = \begin{bmatrix} \epsilon & \gamma & \kappa \end{bmatrix}^T$, we can maintain the structure of Eq. (2.12) and express all fields involved in matrix notation, as

[1] See equations (15) in [1]

follows:

$$\vec{\boldsymbol{d}}' = \mathrm{R}\vec{\boldsymbol{q}} + \vec{\boldsymbol{e}}_1 - \vec{\boldsymbol{E}}_1 \tag{2.14}$$

Strain-displacement equations as represented in Eq. (2.14) will be subsequently utilized in the formulation of the beam model.

2.3 Nonlinear Programming Formulation

The hybrid beam element discretization is presented by utilizing the underlying variational structure of the static problem. The minimizing principle for the TPE is recast here in an NLP formulation and the strain-displacement equations in (2.14) are incorporated, representing the equality constraints of the problem.

2.3.1 NLP framework

The NLP problem adopted herein is of the following form:

$$\begin{aligned} &\text{minimize} && f(\vec{\boldsymbol{x}}) \\ &\text{subject to} && \vec{\boldsymbol{h}}(\vec{\boldsymbol{x}}) = \vec{\mathbf{0}} \\ & && \vec{\boldsymbol{x}} \in \mathcal{S} \end{aligned} \tag{2.15}$$

The objective function $f(\vec{\boldsymbol{x}})$ represents the total potential energy of the structure, whereas vector $\vec{\boldsymbol{h}}(\vec{\boldsymbol{x}})$ includes the active constraints of the program. The corresponding Lagrangian is:

$$\mathcal{L}(\vec{\boldsymbol{x}}, \vec{\boldsymbol{\lambda}}) = f(\vec{\boldsymbol{x}}) + \vec{\boldsymbol{\lambda}}^T \vec{\boldsymbol{h}}(\vec{\boldsymbol{x}}) \tag{2.16}$$

where $\vec{\boldsymbol{\lambda}}$ are the Lagrange multipliers. The first-order optimality conditions are given from the following expression:

$$\nabla \mathcal{L} = \vec{\mathbf{0}} \tag{2.17}$$

This is the standard form of a nonlinear constrained minimization program with equality constraints, as encountered in the literature (e.g. [9]).

2.3.2 Total potential energy

We consider the following decomposition of the total potential energy of a beam:

$$\Pi = U - W \tag{2.18}$$

where U and W are the stored strain energy and potential energy associated with external loading respectively. For the case of concentrated external loads, Eq. (2.18) can be expressed as:

$$\Pi = \int_0^{\ell} \mathcal{W}_S(X_1, \vec{\boldsymbol{q}})\, dX_1 - \sum_{i=1}^{2} \vec{\boldsymbol{P}}_i^T \vec{\boldsymbol{u}}_i \tag{2.19}$$

where $\mathcal{W}_S$ is the strain energy density of a cross section at X_1 and $\vec{\boldsymbol{q}}$ denotes the neutral axis strain vector, $\vec{\boldsymbol{P}}_i$,$\vec{\boldsymbol{u}}_i$ the element nodal force and displacement vectors, respectively. It can be proven[10] that for strain hardening materials within the premises of small strain elastoplasticity, the exact solution to the problem renders Π an absolute minimum. Equivalently, the exact solution solves the program in Eq. (2.15) for $f = \Pi$ with $\vec{\boldsymbol{h}}$ acting as constraints. Assuming a stable work-hardening material, the corresponding Euler-Lagrange equations yield the constitutive equations of elastoplasticity (e.g. see discussion in Simo and Hughes [11]). As it will be shown in subsequent sections, since the constitutive update is carried out locally at the section fiber level.

Section stress resultants are then given by the gradient of $\mathcal{W}_S$:

$$\vec{\boldsymbol{F}}_{sec} = \nabla_{\mathbf{q}} \mathcal{W}_S \tag{2.20}$$

with $\vec{\boldsymbol{F}}_{sec} = \begin{bmatrix} N & V & M \end{bmatrix}^T$. In the case of linear elasticity, the energy density is given by $\mathcal{W}_S = \frac{1}{2}[EA\epsilon^2 + GA_s\gamma^2 + EI\kappa^2]$ and the section resultants are:

$$\vec{\boldsymbol{F}}_{sec} = \begin{bmatrix} EA\epsilon \\ GA_s\gamma \\ EI\kappa \end{bmatrix}$$

where A_s is the effective shear area of the cross-section. Numerical approximation of Eq. (2.19) by an appropriate quadrature yields:

$$f(\vec{\boldsymbol{q}}_1, \ldots, \vec{\boldsymbol{q}}_n, \vec{\boldsymbol{u}}_1, \ldots \vec{\boldsymbol{u}}_N) = \sum_{i=1}^{n} w_i \mathcal{W}_{S,i} - \sum_{i=1}^{2} \vec{\boldsymbol{P}}_i^T \vec{\boldsymbol{u}}_i \tag{2.21}$$

with w_i and n being the weights and the number of integration points respectively, and $\mathcal{W}_{S,i} = \mathcal{W}_S(\vec{\boldsymbol{q}}_i)$. Eq. (2.21) serves as the objective function of the NLP of Eq. (2.15).

2.3.3 Strain-Displacement Constraints

The constrained conditions are derived by applying the same quadrature rule on the integral form of the strain-displacement equations (2.14):

$$\vec{\boldsymbol{d}}(\ell) - \vec{\boldsymbol{d}}(0) = \int_0^\ell \vec{\boldsymbol{d}}' \, dX_1 = \int_0^\ell \mathbf{R}\vec{\boldsymbol{q}} + \vec{\boldsymbol{e}}_1 - \vec{\boldsymbol{E}}_1 \, dX_1 \tag{2.22}$$

Using Eq. (2.4), numerical approximation of the right-hand side integral leads to the element specific constraints:

$$\vec{\boldsymbol{h}}^A = \vec{\boldsymbol{d}}(\ell) - \vec{\boldsymbol{d}}(0) - \sum_{i=1}^{n} w_i \mathbf{R}_i(\vec{\boldsymbol{q}}_i + \vec{\boldsymbol{E}}_1) + \ell\vec{\boldsymbol{E}}_1 = \vec{\mathbf{0}} \tag{2.23}$$

The component form of Eq. (2.23) can be given as:

$$\vec{\boldsymbol{h}}^A = \begin{bmatrix} u(\ell) - u(0) - \sum_{i=1}^{n} w_i \Big[(\epsilon_i + 1)\cos\phi_i - \gamma_i \sin\phi_i\Big] + \ell \\ v(\ell) - v(0) - \sum_{i=1}^{n} w_i \Big[(\epsilon_i + 1)\sin\phi_i + \gamma_i \cos\phi_i\Big] \\ \phi(\ell) - \phi(0) - \sum_{i=1}^{n} w_i \kappa_i \end{bmatrix} \tag{2.24}$$

Although the strain fields appear explicitly only in the weighted evaluation points of the quadrature, the rotational field ϕ is involved in both the integration points and the element edge nodes. As such, we introduce a Lagrange interpolation scheme for the curvature field in the same fashion as in [12]:

$$\kappa(\xi) = \sum_{i=1}^{n} L_i(\xi)\kappa_i \tag{2.25}$$

where L_i are the Lagrange cardinal functions:

$$L_i(\xi) = \frac{\prod_{j=1, j\neq i}^{n} (\xi - \xi_j)}{\prod_{j=1, j\neq i}^{n} (\xi_i - \xi_j)}, \quad \xi = \frac{X_1}{\ell}$$

Substitution of Eq. (2.25) to Eq. (2.13c) yields the expression for rotations ϕ_i:

$$\phi_i - \phi(0) = \sum_{j=1}^{n} \left(\int_0^{\xi_i} L_j(x)\, dx \right) \kappa_j = \sum_{i=1}^{n} T_{ij}\kappa_j \tag{2.26}$$

with derivation of T_{ij} illustrated in Fig. (2.2). In matrix form, the above equation can be directly restated as a linear equality constraint set as:

$$\vec{\boldsymbol{h}}^B = \vec{\boldsymbol{\phi}} - \phi(0)\vec{\mathbf{1}} - \mathbf{T}\vec{\boldsymbol{\kappa}} = \vec{\mathbf{0}} \tag{2.27}$$

where

$$\vec{\boldsymbol{\phi}} = \begin{bmatrix} \phi_1 & \phi_2 & \cdots & \phi_n \end{bmatrix}^T \quad , \vec{\mathbf{1}} = \begin{bmatrix} 1 & 1 & \cdots & 1 \end{bmatrix}^T \in \mathbb{R}^n$$

$$\mathbf{T} = L \begin{bmatrix} \xi_1 & \frac{\xi_1^2}{2} & \cdots & \frac{\xi_1^n}{n} \\ \vdots & \vdots & \ddots & \vdots \\ \xi_n & \frac{\xi_n^2}{2} & \cdots & \frac{\xi_n^n}{n} \end{bmatrix} \boldsymbol{\Theta}^{-1} \quad , \boldsymbol{\Theta} = \begin{bmatrix} 1 & \xi_1 & \xi_1^2 & \cdots & \xi_1^{n-1} \\ \vdots & \vdots & \ddots & \vdots & \\ 1 & \xi_n & \xi_n^2 & \cdots & \xi_n^{n-1} \end{bmatrix}$$

We can then collect all active constraints, Eqs. (2.23),(2.27), in one vector $\vec{\boldsymbol{h}}$:

$$\vec{\boldsymbol{h}} = \begin{bmatrix} \vec{\boldsymbol{h}}^A \\ \vec{\boldsymbol{h}}^B \end{bmatrix} = \begin{bmatrix} \vec{\mathbf{0}} \\ \vec{\mathbf{0}} \end{bmatrix} \tag{2.28}$$

containing all constraints pertaining to one element. While vector $\vec{\boldsymbol{h}}^A$ of strain-displacement constraints will always contain three components for each element, the number of components in vector $\vec{\boldsymbol{h}}^B$ will depend on the chosen quadrature rule.

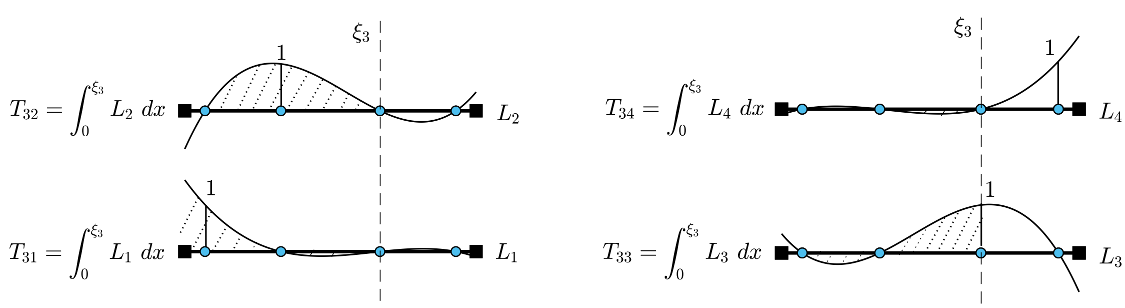

Fig. 2.2. Integration of curvature shape functions.

2.3.4 Lagrangian function

In order to derive the Lagrangian function in the form of Eq. (2.16), we introduce a vector $\vec{\boldsymbol{\lambda}}$ of additional Lagrange multiplier variables and augment Eq. (2.21) with Eq. (2.28):

$$\mathcal{L} = f + \vec{\boldsymbol{\lambda}}^T \vec{\boldsymbol{h}} \tag{2.29}$$

A more convenient form for the Lagrangian function can also be achieved by expanding f into its constituents, namely, the element stored energy and the potential energy:

$$\mathcal{L} = \sum_{e=1}^{n_{el}} U^e - W + \vec{\boldsymbol{\lambda}}^T \vec{\boldsymbol{h}} \tag{2.30}$$

where:

$$U^e = \sum_{i=1}^{n} w_i \mathcal{W}_{S,i}^e \quad , \quad W = \sum_{i=1}^{N} \vec{\boldsymbol{P}}_i^T \vec{\boldsymbol{u}}_i$$

Thereby, additional elements can be simply incorporated by adding their stored energy in the corresponding sum, and considering element constraints by augmenting vectors $\vec{\boldsymbol{\lambda}}$, $\vec{\boldsymbol{h}}$, after transforming them to the global system. Potential function W is "global" in the sense that external loads and the corresponding work-conjugate displacement degrees of freedom are directly added to the expression and are not influenced by adding nodal contributions from adjacent elements. As a result, no additional connectivity constraints at the element interfaces are needed, and Eq. (2.30) is thus a global function for the whole structure.

2.4 Implementation

The set of vectors associated with internal field variables, $\{\vec{\boldsymbol{y}}_i\}_{i=1}^n$, is defined as $\vec{\boldsymbol{y}}_i = \begin{bmatrix} \vec{\boldsymbol{q}}_i & \phi_i \end{bmatrix}^T = \begin{bmatrix} \epsilon_i & \gamma_i & \kappa_i & \phi_i \end{bmatrix}^T$. Moreover, and according to Fig. (2.3), we designate the local element edge degrees of freedom in vector form as $\hat{\boldsymbol{d}}_l = \vec{\boldsymbol{d}}(0)$ and $\hat{\boldsymbol{d}}_r = \vec{\boldsymbol{d}}(\ell)$. The element displacement vector is thus $\hat{\boldsymbol{d}} = \begin{bmatrix} \hat{\boldsymbol{d}}_l^T & \hat{\boldsymbol{d}}_r^T \end{bmatrix}^T$. The corresponding global displacement vector $\vec{\boldsymbol{d}}_g$ is related to the local vector $\hat{\boldsymbol{d}}$ via the typical linear transformation $\boldsymbol{\Lambda}$:

$$\hat{\boldsymbol{d}} = \begin{bmatrix} \boldsymbol{\Lambda} & \mathbf{0} \\ \mathbf{0} & \boldsymbol{\Lambda} \end{bmatrix} \vec{\boldsymbol{d}}_g \quad , \quad \boldsymbol{\Lambda} = \begin{bmatrix} \cos\theta & \sin\theta & 0 \\ -\sin\theta & \cos\theta & 0 \\ 0 & 0 & 1 \end{bmatrix} \tag{2.31}$$

The element constraints of Eqs. (2.23),(2.27) transformed in the global system become:

$$\vec{\boldsymbol{h}}_g^A = \mathbf{V}_1 \vec{\boldsymbol{d}}_g - \boldsymbol{\Lambda}^T \left[\sum_{i=1}^{n} w_i \mathbf{R}_i (\vec{\boldsymbol{q}}_i + \vec{\boldsymbol{E}}_1) - \ell \vec{\boldsymbol{E}}_1 \right] \tag{2.32a}$$

$$\vec{\boldsymbol{h}}_g^B = \vec{\boldsymbol{\phi}} - \mathbf{V}_2 \vec{\boldsymbol{d}}_g - \mathbf{T} \vec{\boldsymbol{\kappa}} \tag{2.32b}$$

where:

$$\mathbf{V}_1 = \begin{bmatrix} -\mathbf{I} & \mathbf{I} \end{bmatrix} \quad , \quad \mathbf{V}_2 = \begin{bmatrix} \vec{\mathbf{0}} & \vec{\mathbf{0}} & \vec{\mathbf{1}} & \vec{\mathbf{0}} & \vec{\mathbf{0}} & \vec{\mathbf{0}} \end{bmatrix}$$

$$\mathbf{I} = \begin{bmatrix} 1 & 0 & 0 \\ 0 & 1 & 0 \\ 0 & 0 & 1 \end{bmatrix} \quad , \quad \vec{\mathbf{0}} \in \mathbb{R}^n$$

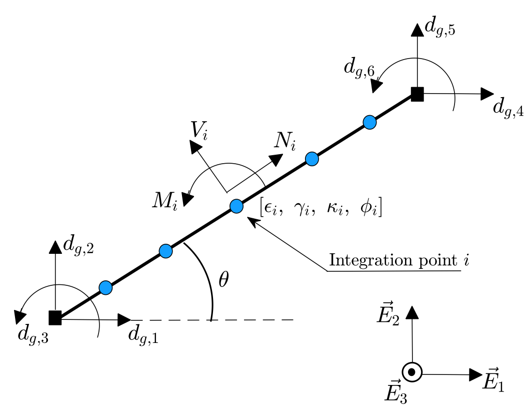

Fig. 2.3. Typical element representing one member.

In the equation above the superscript denoting an element is ommited for clarity. The element contribution to the Lagrangian of the assemblage, denoted $\mathcal{E}^e$, is then:

$$\mathcal{E}^e(\vec{\boldsymbol{y}}_1, \dots \vec{\boldsymbol{y}}_n, \vec{\boldsymbol{d}}_g, \vec{\boldsymbol{\lambda}}^e) = U^e + (\vec{\boldsymbol{\lambda}}^e)^T \vec{\boldsymbol{h}}_g^e \tag{2.33}$$

Notice that the external potential function W is not included in Eq. (2.33) as it is added directly via the work done by external forces in the global degrees of freedom and not from element contributions. The element Lagrange multipliers $\vec{\boldsymbol{\lambda}}^e$ are force conjugate measures at the corresponding degrees of freedom and U^e is the sum total of cross-section strain energies. The Lagrangian of the whole system is accordingly given by:

$$\mathcal{L}(\vec{\boldsymbol{y}}, \vec{\boldsymbol{d}}_g, \vec{\boldsymbol{\lambda}}) = U - W + \vec{\boldsymbol{\lambda}}^T \vec{\boldsymbol{h}}_g \tag{2.34}$$

which is a restatement of Eq. (2.30) in the global coordinate system and $\vec{\boldsymbol{y}} = \begin{bmatrix} \vec{\boldsymbol{y}}_1^T & \vec{\boldsymbol{y}}_2^T & \cdots & \vec{\boldsymbol{y}}_m^T \end{bmatrix}^T$, with m being the total number of quadrature points in in the structure.

2.4.1 Equilibrium

In what follows, it is assumed we are dealing with quantities pertaining to the total assemblage, after all element contributions have been resolved. The first-order necessary optimality condition for the Lagrangian function (see Eq. (2.17)), after the imposition of boundary conditions, yields the following relations:

$$\nabla_{\mathbf{y}_i} \mathcal{L} = \nabla_{\mathbf{y}_i} U + [\nabla_{\mathbf{y}_i} \vec{\boldsymbol{h}}_g] \vec{\boldsymbol{\lambda}} = \vec{\mathbf{0}} \tag{2.35a}$$

$$\nabla_{\mathbf{d}_g} \mathcal{L} = -\nabla_{\mathbf{d}_g} W + [\nabla_{\mathbf{d}_g} \vec{\boldsymbol{h}}_g] \vec{\boldsymbol{\lambda}} = \vec{\mathbf{0}} \tag{2.35b}$$

$$\nabla_{\lambda} \mathcal{L} = \vec{\boldsymbol{h}}_g = \vec{\mathbf{0}} \tag{2.35c}$$

Eq. (2.35a) expresses the equilibrium between external and internal forces acting on the i-th cross-section for $i = 1, 2, \dots m$, while Eq. (2.35b) ensures consistency between externally applied loads and Lagrange multipliers. Finally, Eq. (2.35c) requires that all constraints are active when the minimum is attained. Explicit expressions for the first and second derivatives of all quantities involved are given in the Appendix. We should note that derivatives of the strain energy U are computed numerically during the cross-section state determination phase in Sec. (2.4.3).

2.4.2 Hessian matrix

The Hessian matrix of the Lagrangian function contains second order information of the system and is utilized during the solution phase. Eqs. (2.35a)-(2.35c) constitute a set of nonlinear algebraic equations and an iterative scheme is needed to solve the system. In block matrix form, the Hessian is provided as:

$$\mathbf{H} = \begin{bmatrix} \nabla^2_{\mathbf{yy}}\mathcal{L} & \nabla^2_{\mathbf{yd_g}}\mathcal{L} & \nabla^2_{\mathbf{y}\lambda}\mathcal{L} \\ \nabla^2_{\mathbf{yd_g}}\mathcal{L}^T & \nabla^2_{\mathbf{d_g d_g}}\mathcal{L} & \nabla^2_{\mathbf{d_g}\lambda}\mathcal{L} \\ \nabla^2_{\mathbf{y}\lambda}\mathcal{L}^T & \nabla^2_{\mathbf{d_g}\lambda}\mathcal{L}^T & \nabla^2_{\lambda\lambda}\mathcal{L} \end{bmatrix} = \begin{bmatrix} \nabla^2_{\mathbf{yy}}\mathcal{L} & \mathbf{0} & \nabla_{\mathbf{y}}\vec{\boldsymbol{h}}_g^T \\ \mathbf{0} & \mathbf{0} & \nabla_{\mathbf{d_g}}\vec{\boldsymbol{h}}_g^T \\ \nabla_{\mathbf{y}}\vec{\boldsymbol{h}}_g & \nabla_{\mathbf{d_g}}\vec{\boldsymbol{h}}_g & \mathbf{0} \end{bmatrix} \tag{2.36}$$

The resulting Hessian is fairly sparse. Moreover, the block matrix $\nabla_{\mathbf{yy}}U$ which contains section stiffness information is block-diagonal (see Appendix B) and its symmetry guarantees the full symmetry of $\mathbf{H}$.

2.4.3 Solution scheme

As mentioned in Appendix B, the nonlinear system of equations in Eq. (2.17) is solved in an incremental-iterative fashion. Linearization around the current iteration k yields:

$$\nabla\mathcal{L}^k + \mathbf{H}^k\delta\vec{\boldsymbol{z}}^k = \vec{\mathbf{0}} \tag{2.37}$$

where $\vec{\boldsymbol{z}}$ is the vector of all unknowns:

$$\vec{\boldsymbol{z}} = \begin{bmatrix} \vec{\boldsymbol{y}} \\ \vec{\boldsymbol{d}}_g \\ \vec{\boldsymbol{\lambda}} \end{bmatrix}, \quad \text{with} \quad \vec{\boldsymbol{y}} = \begin{bmatrix} \vec{\boldsymbol{y}}_1 \\ \vdots \\ \vec{\boldsymbol{y}}_m \end{bmatrix}$$

Reference to the current iteration step is omitted subsequently for clarity. Solving Eq. (2.37) directly may be cumbersome in some cases, especially for problems that require denser distribution of integration points (e.g. plasticity), since the Hessian is not banded and may also be badly conditioned. In addition, implementation of continuation schemes in order to attain solutions past critical points is more involved since the state variable vector contains displacements, strains and Lagrange multiplier unknowns. A different approach is hence sought, where the initial linear system is reduced to a smaller one involving only the displacement vector $\vec{\boldsymbol{d}}_g$. Restating the system in terms of its distinct vector components $\vec{\boldsymbol{y}}$, $\vec{\boldsymbol{d}}_g$ and $\vec{\boldsymbol{\lambda}}$ gives:

$$\begin{bmatrix} \nabla_{\mathbf{y}}\mathcal{L} \\ \nabla_{\mathbf{d}_g}\mathcal{L} \\ \nabla_{\lambda}\mathcal{L} \end{bmatrix} + \begin{bmatrix} \nabla^2_{\mathbf{yy}}\mathcal{L} & 0 & \nabla_{\mathbf{y}}\vec{\boldsymbol{h}}_g^T \\ 0 & 0 & \nabla_{\mathbf{d}_g}\vec{\boldsymbol{h}}_g^T \\ \nabla_{\mathbf{y}}\vec{\boldsymbol{h}}_g & \nabla_{\mathbf{d}_g}\vec{\boldsymbol{h}}_g & 0 \end{bmatrix} \begin{bmatrix} \delta\vec{\boldsymbol{y}} \\ \delta\vec{\boldsymbol{d}}_g \\ \delta\vec{\boldsymbol{\lambda}} \end{bmatrix} = \begin{bmatrix} \vec{0} \\ \vec{0} \\ \vec{0} \end{bmatrix} \tag{2.38}$$

Utilizing Eqs. (2.35a)-(2.35c) and setting $\delta\vec{\boldsymbol{\lambda}} = \vec{\boldsymbol{\lambda}}^{k+1} - \vec{\boldsymbol{\lambda}}^k$, Eq. (2.38) can be rewritten as:

$$\begin{bmatrix} \nabla_{\mathbf{y}}U \\ -\vec{\boldsymbol{P}} \\ \vec{\boldsymbol{h}}_g \end{bmatrix} + \begin{bmatrix} \nabla^2_{\mathbf{yy}}\mathcal{L} & 0 & \nabla_{\mathbf{y}}\vec{\boldsymbol{h}}_g^T \\ 0 & 0 & \nabla_{\mathbf{d}_g}\vec{\boldsymbol{h}}_g^T \\ \nabla_{\mathbf{y}}\vec{\boldsymbol{h}}_g & \nabla_{\mathbf{d}_g}\vec{\boldsymbol{h}}_g & 0 \end{bmatrix} \begin{bmatrix} \delta\vec{\boldsymbol{y}} \\ \delta\vec{\boldsymbol{d}}_g \\ \vec{\boldsymbol{\lambda}}_{k+1} \end{bmatrix} = \begin{bmatrix} \vec{0} \\ \vec{0} \\ \vec{0} \end{bmatrix} \tag{2.39}$$

As mentioned previously, the gradient of the strain energy with respect to the strain vector represents the cross-sectional stress resultants. Solving the first equation in the system of

Eq. (2.39) for $\delta\vec{\boldsymbol{y}}$ we get:

$$\delta\vec{\boldsymbol{y}} = -\nabla^2_{\mathbf{yy}}\mathcal{L}^{-1}\left[\vec{\boldsymbol{F}}_{sec} + \nabla_{\mathbf{y}}\vec{\boldsymbol{h}}_g^T\vec{\boldsymbol{\lambda}}_{k+1}\right] \tag{2.40}$$

Substituting Eq. (2.40) in the third equation of Eq. (2.39) and solving for $\vec{\boldsymbol{\lambda}}^{k+1}$ yields:

$$\vec{\boldsymbol{\lambda}}^{k+1} = \mathbf{B}^{-1}[\vec{\boldsymbol{h}}_g - \vec{\boldsymbol{b}}] + \mathbf{B}^{-1}[\nabla_{\mathbf{d}_g}\vec{\boldsymbol{h}}_g]\delta\vec{\boldsymbol{d}}_g \tag{2.41}$$

By substituting Eq. (2.41) into the second system equation Eq. (2.35b) we arrive at the familiar static equilibrium form of the system of equations:

$$\mathbf{K}\delta\vec{\boldsymbol{d}}_g = \vec{\boldsymbol{P}} - \vec{\boldsymbol{F}}_{int} \tag{2.42}$$

which can now be solved for the iterative displacement vector $\delta\vec{\boldsymbol{d}}_g$. Vectors $\vec{\boldsymbol{b}}$, $\vec{\boldsymbol{F}}_{int}$ and matrices $\mathbf{B}$, $\mathbf{K}$, are given by the following explicit formulas in the global system:

$$\vec{\boldsymbol{b}} = [\nabla_{\mathbf{y}}\vec{\boldsymbol{h}}_g][\nabla^2_{\mathbf{yy}}\mathcal{L}]^{-1}\vec{\boldsymbol{F}}_{sec} \tag{2.43a}$$

$$\vec{\boldsymbol{F}}_{int} = [\nabla_{\mathbf{d}_g}\vec{\boldsymbol{h}}_g]^T[\mathbf{B}]^{-1}[\vec{\boldsymbol{h}}_g - \vec{\boldsymbol{b}}] \tag{2.43b}$$

$$\mathbf{B} = [\nabla_{\mathbf{y}}\vec{\boldsymbol{h}}_g][\nabla^2_{\mathbf{yy}}\mathcal{L}]^{-1}[\nabla_{\mathbf{y}}\vec{\boldsymbol{h}}_g]^T \tag{2.43c}$$

$$\mathbf{K} = [\nabla_{\mathbf{d}_g}\vec{\boldsymbol{h}}_g]^T[\mathbf{B}]^{-1}[\nabla_{\mathbf{d}_g}\vec{\boldsymbol{h}}_g] \tag{2.43d}$$

where $\vec{\boldsymbol{b}} \in \mathbb{R}^p$, $\vec{\boldsymbol{F}}_{int} \in \mathbb{R}^{3N}$, N is again the number of structural nodes, $\mathbf{B} \in \mathbb{R}^{p\times p}$ with $p = m + 3n_{nel}$, and $\mathbf{K} \in \mathbb{R}^{3N\times 3N}$.

Equivalently, an assembly process can also be implemented by casting Eqs. (2.43a), (2.43c) in local form, where they can be further simplified by being expanded in terms of element cross-section contributions:

$$\vec{\boldsymbol{b}}^e = \sum_{i=1}^{n} [\nabla_{\mathbf{y}_i} \vec{\boldsymbol{h}}_g][\nabla^2_{\mathbf{y}_i \mathbf{y}_i} \mathcal{L}]^{-1} \vec{\boldsymbol{F}}^{(i)}_{sec} \tag{2.44a}$$

$$\mathbf{B}^e = \sum_{i=1}^{n} [\nabla_{\mathbf{y}_i} \vec{\boldsymbol{h}}_g][\nabla^2_{\mathbf{y}_i \mathbf{y}_i} \mathcal{L}]^{-1} [\nabla_{\mathbf{y}_i} \vec{\boldsymbol{h}}_g]^T \tag{2.44b}$$

where n is the number of element quadrature points, $\vec{\boldsymbol{b}}^e \in \mathbb{R}^{n+3}$ and $\mathbf{B}^e \in \mathbb{R}^{(n+3)\times(n+3)}$. The element stiffness matrix $\mathbf{K}^e \in \mathbb{R}^{6\times 6}$ and internal force vector $\vec{\boldsymbol{F}}^e_{int} \in \mathbb{R}^6$ are given by the same expressions as in Eqs. (2.43b), (2.43d), but with the gradients now cast in the local element form. For the assembly, the standard FEM routines can be directly employed and the resulting global stiffness operator retains all properties typically associated with it in the context of classical finite element analysis, i.e. it is a symmetric positive definite matrix, it is well-conditioned and, importantly, it is sparse and banded. Hence, in this case, the global internal force vector and the global stiffness matrix are given by the standard assembly process, designated here via operator Λ:

$$\vec{\boldsymbol{F}}_{int} = \bigwedge_{e=1}^{n_{el}} \vec{\boldsymbol{F}}^e_{int} \tag{2.45}$$

$$\mathbf{K} = \bigwedge_{e=1}^{n_{el}} \mathbf{K}^e \tag{2.46}$$

with

$$\vec{\boldsymbol{F}}^e_{int} = [\nabla_{\mathbf{d}_g} \vec{\boldsymbol{h}}^e_g]^T [\mathbf{B}^e]^{-1} [\vec{\boldsymbol{h}}^e_g - \vec{\boldsymbol{b}}^e] \tag{2.47}$$

$$\mathbf{K}^e = [\nabla_{\mathbf{d}_g} \vec{\boldsymbol{h}}^e_g]^T [\mathbf{B}^e]^{-1} [\nabla_{\mathbf{d}_g} \vec{\boldsymbol{h}}^e_g] \tag{2.48}$$

where $\vec{\boldsymbol{h}}^e_g \in \mathbb{R}^{n+3}$ denotes the *element* constraint vector given by Eq. (2.28) and $\nabla_{\mathbf{d}_g} \vec{\boldsymbol{h}}^e_g \in \mathbb{R}^{(n+3)\times 6}$ its gradient with respect to the global displacement degrees of freedom (DOFs) associated with it, is given in Appendix A. It is clear that with this formulation the inversion of large global matrices for the computation of $\mathbf{K}$ and $\vec{\boldsymbol{F}}_{int}$ is avoided and, instead, only inversion of the local elements flexibility matrices $\mathbf{B}^e$ is required. Given that for highly nonlinear problems we typically have $n \in \mathbb{N}([5, 10])$ for satisfactory accuracy, this results in an element flexibility matrix of dimension $\dim(\mathbf{B}^e) \leq 13$, thus accelerating the analysis considerably.

Having written the system of equations in the form of Eq. (2.42), implementation of arc-length type schemes is now straighforward. In the present work, we adopt the algorithm proposed by Crisfield [13] whereby the additional equation supplemented to the system is:

$$\Delta\vec{\boldsymbol{d}}_g^T \Delta\vec{\boldsymbol{d}}_g = \Delta S^2 \tag{2.49}$$

with ΔS being the user-specified arc-length parameter. The incremental displacement vector $\Delta\vec{\boldsymbol{d}}_g$ is updated in each iteration as follows:

$$\Delta\vec{\boldsymbol{d}}_g^k = \Delta\vec{\boldsymbol{d}}_g^{k-1} + \delta\vec{\boldsymbol{d}}_g^k \tag{2.50}$$

where k denotes the current iteration and $\delta\vec{\boldsymbol{d}}_g^k$ is the vector of iterative displacements.

Solution updating

After the determination, at an arbitrary iteration k within step j, of the iterative displacement vector $\delta\vec{\boldsymbol{d}}_g^k$ from Eq. (2.42), the strain and Lagrange multiplier vectors in Eqs. (2.40),(2.41) have then to be updated. The detailed steps of the updating procedure are as follows:

Step j, iteration k: $\left\{ \vec{\boldsymbol{y}}_j^0, \quad \vec{\boldsymbol{d}}_{g,j}^0, \quad \vec{\boldsymbol{\lambda}}_j^0, \quad \vec{\boldsymbol{P}}_j, \quad \Delta\vec{\boldsymbol{y}}_j^{k-1}, \quad \Delta\vec{\boldsymbol{d}}_{g,j}^{k-1} \right\}$

(1): Get section stiffnesses $\nabla^2_{\mathbf{yy}}\mathcal{L}^k$ from Eq. (B.3) in Appendix B and section forces $\vec{\boldsymbol{F}}_{sec}^k$ from section integration, Eq. (2.55).

(2): Evaluate $\vec{\boldsymbol{b}}^k$ and B^k from Eqs. (2.43a), (2.43c) respectively (or, alternatively, $\vec{\boldsymbol{b}}^{e\ k}$, $\mathrm{B}^{e\ k}$ from Eqs. (2.44a), (2.44b)).

(3): Evaluate $\mathbf{K}^k$ from Eq. (2.43d), (or, alternatively, from Eqs. (2.46), (2.48)).

(4): Solve Eq. (2.42) for $\delta\vec{\boldsymbol{d}}_g^k$.

(5): Update incremental displacement vector: $\Delta\vec{\boldsymbol{d}}_{g,j}^k \leftarrow \Delta\vec{\boldsymbol{d}}_{g,j}^{k-1} + \delta\vec{\boldsymbol{d}}_g^k$

(6): Update displacement vector: $\vec{\boldsymbol{d}}_{g,j}^k \leftarrow \vec{\boldsymbol{d}}_{g,j}^0 + \Delta\vec{\boldsymbol{d}}_g^k$

(7): Update Langrange multiplier $\vec{\boldsymbol{\lambda}}_j^k$ from Eq. (2.41).

(8): Evaluate iterative strain vector $\delta\vec{\boldsymbol{y}}^k$ from Eq. (2.40).

(9): Update incremental strain vector: $\Delta\vec{\boldsymbol{y}}_j^k \leftarrow \Delta\vec{\boldsymbol{y}}_j^{k-1} + \delta\vec{\boldsymbol{y}}^k$

(10): Update total strain vector: $\vec{\boldsymbol{y}}_j^k \leftarrow \vec{\boldsymbol{y}}_j^0 + \Delta\vec{\boldsymbol{y}}_j^k$

(11): Evaluate $\vec{\boldsymbol{F}}_{int}^k$ from Eq. (2.43b) (or, alternatively, from Eqs. (2.45), (2.47)).

(12): Check $\|\vec{\boldsymbol{P}}_j - \vec{\boldsymbol{F}}_{int}^k\| \leq \mathrm{tol} \cdot \|\vec{\boldsymbol{P}}_j - \vec{\boldsymbol{F}}_{int}^0\|$.

(13): If **FALSE**, set $k \leftarrow k+1$ and go to **(1)**. If **TRUE**, set $j \leftarrow j+1$, $\vec{\boldsymbol{y}}_j^0 \leftarrow \vec{\boldsymbol{y}}_{j-1}^k$, $\vec{\boldsymbol{d}}_{g,j}^0 \leftarrow \vec{\boldsymbol{d}}_{g,j-1}^k$, $\vec{\boldsymbol{\lambda}}_j^0 \leftarrow \vec{\boldsymbol{\lambda}}_{j-1}^k$.

2.4.4 Cross-section state determination

During the updating scheme described in the previous section, the section stress resultants $\vec{\boldsymbol{F}}_{sec}$, along with the matrix $\nabla^2_{\mathbf{yy}}\mathcal{L}$, are required. The latter, as seen subsequently, corresponds to the generalized section stiffnesses. In the general case where inelastic behavior is considered, the stress-strain constitutive law has to be integrated at the cross-section level and the material properties have to be updated accordingly. In this work, each cross-section is discretized in n_l number of layers and the stress update is performed independently for each layer. This is equivalent to the composite midpoint rule applied along the height of the cross-section. The shear coefficient k_s is introduced as a correction factor for the simplifying aforementioned assumption, in accordance with Cowper [14].

Below we present the kinematic and constitutive relations for a cross-section object. The (multiaxial) constitutive law at the fiber level is treated in the next chapter. The update procedure is regarded as strain-driven, in the sense that the known initial state is updated given an increment in the centerline strains at a particular quadrature point. First, we define the stress and strain vectors associated with a particular fiber:

$$\vec{\boldsymbol{\sigma}}_f = \begin{bmatrix} \sigma_{11} & \sigma_{12} \end{bmatrix}^T, \quad \vec{\boldsymbol{\epsilon}}_f = \begin{bmatrix} \epsilon_{11} & \gamma_{12} \end{bmatrix}^T \tag{2.51}$$

In line with the plane section hypothesis, the fiber strain vector can be determined from the centerline strain vector as follows:

$$\begin{aligned} \epsilon_{11} &= \varepsilon - X_2\kappa \\ \gamma_{12} &= \varphi(X_2)\gamma \end{aligned} \iff \vec{\boldsymbol{\epsilon}}_f = \mathbf{N}_s\vec{\boldsymbol{q}}, \quad \mathbf{N}_s = \begin{bmatrix} 1 & 0 & -X_2 \\ 0 & \varphi(X_2) & 0 \end{bmatrix} \tag{2.52}$$

where $\varphi(X_2)$ is an as of now unspecified function that defines a shear strain distribution along the height of the cross-section.

Thus, given $\left\{\vec{\boldsymbol{q}}, \quad \vec{\boldsymbol{q}}^{pl}\right\}$, $\Delta\vec{\boldsymbol{q}}$, along with a set of internal state variables (e.g. accumulated plastic strain), we can evaluate the incremental strains at the midpoint of a layer at distance X_2 from the neutral axis as follows:

$$\vec{\boldsymbol{\epsilon}}_f = \mathbf{N}_s\vec{\boldsymbol{q}} \tag{2.53a}$$

$$\Delta\vec{\boldsymbol{\epsilon}}_f = \mathbf{N}_s\Delta\vec{\boldsymbol{q}} \tag{2.53b}$$

where it is reminded that $\vec{\boldsymbol{q}}$ is the vector containing the neutral axis generalized strains and $\vec{\boldsymbol{\epsilon}}_f$ is the strain vector associated with the fiber midpoint. With Eqs. (2.53a), (2.53b) and the initial state known, we can perform the stress update which will yield the updated stress vector $\vec{\boldsymbol{\sigma}}_f$ and the (consistent) elastoplastic modulus for the fiber. The conjugate stress resultants associated with the assumed kinematic assumptions are derived from the element virtual work equation:

$$\vec{\boldsymbol{P}}_l^T \delta \vec{\boldsymbol{d}}_l + \vec{\boldsymbol{P}}_r^T \delta \vec{\boldsymbol{d}}_r = \int_V \vec{\boldsymbol{\sigma}}_f^T \delta \vec{\boldsymbol{\epsilon}}_f \, dV = \int_0^L \left[\int_A \mathbf{N}_s^T \vec{\boldsymbol{\sigma}}_f dA \right]^T \vec{\boldsymbol{q}} \, dX_1 \tag{2.54}$$

where we define the conjugate section stress resultants associated with $\vec{\boldsymbol{q}}$ as follows:

$$\vec{\boldsymbol{F}}_{sec}^{(i)} = \int_A \mathbf{N}_s^T \vec{\boldsymbol{\sigma}}_f \, dA \tag{2.55}$$

Application of the composite midpoint rule on Eq. (2.55) yields:

$$\vec{\boldsymbol{F}}_{sec}^{(i)} \approx \begin{bmatrix} \sum_{j=1}^{n_l} \sigma_{11,j} \Delta A_j \\ \sum_{j=1}^{n_l} \sigma_{12,j} \Delta A_j \\ \sum_{j=1}^{n_l} X_{2,j} \sigma_{11,j} \Delta A_j \end{bmatrix} \tag{2.56}$$

where ΔA_j the area of layer j.

Let $\mathbf{C} = \partial \vec{\boldsymbol{\sigma}}_f / \partial \vec{\boldsymbol{\epsilon}}_f$ designate the tangent modulus at a fiber. During elastic steps, $\mathbf{C} \equiv \mathbf{C}^{el} = \text{diag}[E, G]$. In the next chapter we will see that during plastic steps the diagonal components of $\mathbf{C}$ are, generally, also non-zero. The tangent section stiffness is derived as follows:

$$\mathbf{k}_{sec}^{(i)} = \frac{\partial \vec{\boldsymbol{F}}_{sec}^{(i)}}{\partial \vec{\boldsymbol{q}}} = \int_A \mathbf{N}_s^T \frac{\partial \vec{\boldsymbol{\sigma}}_f}{\partial \vec{\boldsymbol{q}}} \, dA = \int_A \mathbf{N}_s^T \frac{\partial \vec{\boldsymbol{\sigma}}_f}{\partial \vec{\boldsymbol{\epsilon}}_f} \frac{\partial \vec{\boldsymbol{\epsilon}}_f}{\partial \vec{\boldsymbol{q}}} \, dA = \int_A \mathbf{N}_s^T \mathbf{C} \mathbf{N}_s \, dA \tag{2.57}$$

Application of the midpoint rule on Eq. (2.57) yields the following component form for

$\mathbf{k}_s^{(i)}$:

$$\mathbf{k}_{sec}^{(i)} = \begin{bmatrix} C_{11}^i & \varphi^i C_{12}^i & -X_2^i C_{11}^i \\ \varphi^i C_{21}^i & (\varphi^i)^2 C_{22}^i & -x_2^i \varphi^i C_{21}^i \\ -X_2^i C_{11}^i & -x_2^i \varphi^i C_{12}^i & (X_2^i)^2 C_{11}^i \end{bmatrix} \tag{2.58}$$

where C_{ij} are the components of the elastoplastic consistent tangent modulus of the fiber. The section stiffness is then given by the following sum:

$$\mathbf{k}_{sec} = \sum_{i=1}^{n_f} \mathbf{k}_{sec}^{(i)} \Delta A^i \tag{2.59}$$

Given an increment in nodal displacements at the global/structural level, the assembly process has to loop over all elements in order to determine the element stiffness and internal nodal forces. This procedure, illustrated in Fig. 2.4, involves analysis at three different levels: the global/element, the section state determination, and the fiber stress update. Having briefly outlined the basic theory for the hybrid element as it pertains to the first two levels mentioned above, next we introduce the elastoplastic stress update formulation, which pertains to the third level of the solution process and results in a fast return mapping algorithm.

The generalized section stiffness, $\nabla^2_{\mathbf{y}_i\mathbf{y}_i}\mathcal{L}$, is given by the second derivatives of the Lagrangian with respect to strain vector $\vec{\boldsymbol{y}}_i = \begin{bmatrix} \vec{\boldsymbol{q}}_i^T & \phi_i \end{bmatrix}^T$:

$$\nabla^2_{\mathbf{y}_i\mathbf{y}_i}\mathcal{L} = \nabla^2_{\mathbf{y}_i\mathbf{y}_i} U + \nabla_{\mathbf{y}_i}([\nabla_{\mathbf{y}_i} \vec{\boldsymbol{h}}_g]\vec{\boldsymbol{\lambda}}) \tag{2.60}$$

where:

$$\nabla^2_{\mathbf{y}_i\mathbf{y}_i} U = w_i \begin{bmatrix} \mathbf{k}_{sec}^{(i)} & \mathbf{0} \\ \mathbf{0} & 0 \end{bmatrix}$$

For the explicit expression of the second term in the right-hand side of Eq. (2.60), see Ap-

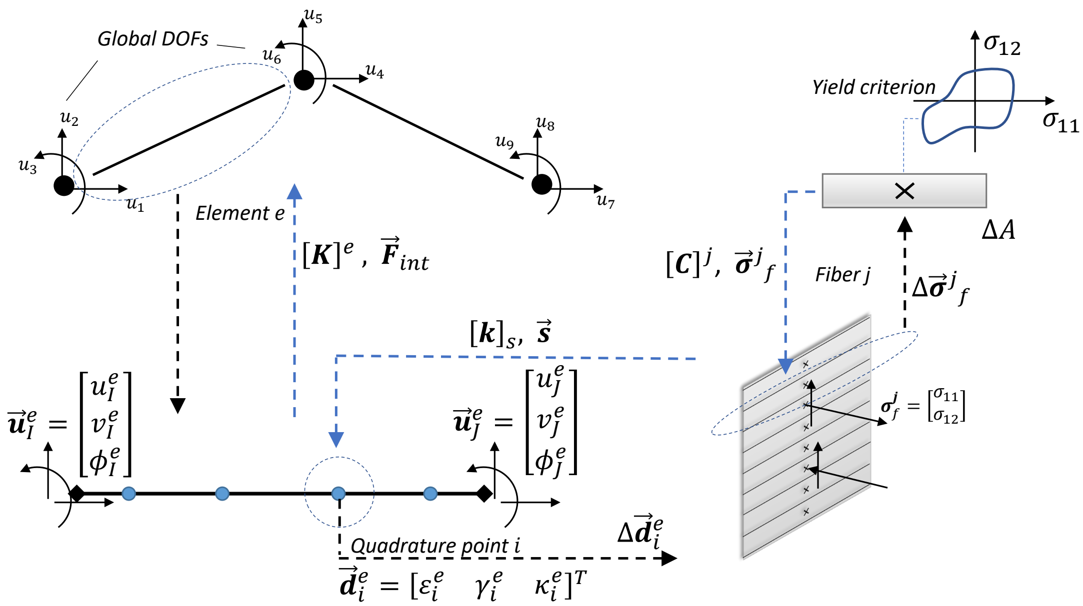

Fig. 2.4. Solutions process stages. Quantities $\mathbf{K}^e$ and $\vec{\boldsymbol{F}}_{int}$ stand for stiffness matrix and internal nodal force vector for element e respectively.

pendix B. It generally includes parameters associated with section rotations and Lagrange multipliers, and is greatly simplified if small displacement assumptions are used.

CHAPTER 3

MATERIAL CONSTITUTIVE MODEL

3.1 Introduction

In this chapter we introduce an algorithm for shear-axial-flexure interaction suited for fibre beam elements of any kind (displacement-based or otherwise). The coupling is taken into account by considering a multiaxial constitutive law at the level of cross-section fibers. Thus, stress resultant interaction as well as the consistent tangent stiffness of a cross-section are derived during the state determination phase. Integration of the elastoplasic rate equations on each fiber is carried out using the fully backward (implicit) Euler method, which as is known, results in the so-called closest point projection algorithm. In addition, the constrained stress state of a fiber is exploited in order to devise a return-mapping scheme that avoids incorporating stress components that are not energetically active. The appropriate mapping on the constrained space is inspirited by the work of Simo[15] and appropriately adapted for fibre discretized elements. This leads to a stress update algorithm that is significantly faster while also requiring less memory requirements for storage of non-active tensor components, compared to formulations that utilize a general three dimensional algorithm[16, 17, 18, 19, 20]. In the latter case, stress update is a nested procedure within an outer Newton iteration which is necessitated in order to enforce the constraint for the transverse stress components, $\sigma_{22} = \sigma_{33} = 0$. This is because during the trial phase of a plastic step, the transverse components become non-zero. Furthermore, a static condensation of the three-dimensional consistent tangent is required to enforce both the local Newton scheme and to derive the consistent tangent modulus pertaining to the fiber stress state. The algorithm introduced in this chapter bypasses the need for additional outer iterations, thereby resulting in a much faster stress update procedure.

For the exposition we adopted the $J2$ consitutive model which is based on the von Mises yield criterion, which is suited for modelling the elastoplastic response of metals. Linear kinematic and general isotropic hardening are incorporated in the formulation. Moreover, infinitesimal strains and a rate-independent associative plasticity framework are the core assumptions that underlie the proposed algorithm. This chapter is subdivided in three main sections: first, we briefly outline the general (rate) form of the three-dimensional elastoplastic equations. In the second section we present the rate constitutive model as it pertains to the fiber stress state and derive expressions for the continuous elastoplastic moduli. Finally, in the third section we outline the implementation details, which are based on application of the fully implicit Euler scheme. In addition we derive the expression for the consistent tangent modulus at a fiber, which is required to ensure quadratic rates of convergence for the global Newton method.

3.1.1 Notation

Furthermore, boldface lowercase letters indicate second order tensor. Wherever the same letters appear with an overhead arrow, this indicates the vector notation for the tensor represented with that letter. The notation adopted herein is the following:

$$\boldsymbol{\sigma} = \begin{bmatrix} \sigma_{11} & \sigma_{12} & \sigma_{13} \\ \sigma_{12} & \sigma_{22} & \sigma_{23} \\ \sigma_{13} & \sigma_{23} & \sigma_{33} \end{bmatrix} \rightarrow \vec{\boldsymbol{\sigma}} = \begin{bmatrix} \sigma_{11} & \sigma_{22} & \sigma_{33} & \sigma_{12} & \sigma_{23} & \sigma_{13} \end{bmatrix}^T$$

For strain tensors, components for which $i \neq j$ are multiplied by 2.

3.2 Three-dimensional Constitutive Model

Below we outline the general rate form of rate-independent elastoplasticity with combined isotropic and linear kinematic hardening. Infinitesimal strains and associateive plasticity are assumed, while the yield criterion is purposefully unspecified at this state in order to maintain generality.

Let $\boldsymbol{\sigma},\ \boldsymbol{\epsilon}$ be the second order symmetric stress and strain tensors. We introduce the internal hardening variables $\boldsymbol{\alpha}$ and q which represent the second order back-stress tensor and the equivalent uniaxial yield stress respectively. The former is associated with kinematic hardening while the latter models isotropic hardening. Finally, consider the decomposition of the strain tensor into elastic and plastic parts as follows:

$$\boldsymbol{\epsilon} = \boldsymbol{\epsilon}^{el} + \boldsymbol{\epsilon}^{pl} \tag{3.1}$$

Then the rate form of the constitutive equations for the assumptions mentioned above is the following:

$$\begin{aligned}
\dot{\boldsymbol{\epsilon}} &= \dot{\boldsymbol{\epsilon}}^{el} + \dot{\boldsymbol{\epsilon}}^{pl} && \text{(Strain decomposition)} && \text{(3.2a)}\\
\dot{\boldsymbol{\sigma}} &= \mathbb{C}^{el}\left[\dot{\boldsymbol{\epsilon}} - \dot{\boldsymbol{\epsilon}}^{pl}\right] && \text{(Elastic constitutive law)} && \text{(3.2b)}\\
\dot{\boldsymbol{\epsilon}}^{pl} &= \dot{\lambda}\frac{\partial \Phi}{\partial \boldsymbol{\sigma}} && \text{(Flow rule)} && \text{(3.2c)}\\
\dot{\boldsymbol{\alpha}} &= -\dot{\lambda} H_{kin}\frac{\partial \Phi}{\partial \boldsymbol{\alpha}} && \text{(Kinematic hardening law)} && \text{(3.2d)}\\
\dot{q} &= \frac{\partial q}{\partial e^{pl}}\dot{e}^{pl} && \text{(Isotropic hardening law)} && \text{(3.2e)}\\
\dot{e}^{pl} &= \dot{\lambda} && \text{(Equivalent plastic strain)} && \text{(3.2f)}\\
\Phi(\boldsymbol{\sigma}, \boldsymbol{\alpha}, e^{pl}) &= \sigma_{eq}(\boldsymbol{\sigma}, \boldsymbol{\alpha}) - q(e^{pl}) \leq 0 && \text{(Yield criterion)} && \text{(3.2g)}
\end{aligned}$$

In the above system of differential algebraic equations, λ is the plastic parameter, H_{kin} is the kinematic hardening modulus, $\mathbb{C}^{el}$ is the elastic moduli, a fourth order tensor, of the material and σ_{eq} is the equivalent stress, which is determined by the yield criterion used. Furthermore, in the case of linear isotropic hardening with modulus H_{iso}, the corresponding harening law (Eq. 3.2e) becomes $\dot{q} = H_{iso}\dot{e}^{pl}$, where e^{pl} is the equivalent plastic strain. Finally, with the inequality in Eq. (3.2g) we define a feasible stress space. Stress points stictly satisfying the inequality, $\Phi < 0$ represent an elastic state while those that cause plastic flow render Φ zero.

The so-called Karush-Kuhn-Tucker loading/unloading conditions derived from the underlying constrained variational problem[21] can be stated as follows:

$$\Phi \leq 0, \qquad \dot{\lambda} \geq 0, \qquad \dot{\lambda}\Phi = 0 \tag{3.3}$$

From these conditions we can determine the current stress state:

- if $\dot{\lambda} > 0$, then $\dot{\lambda}\Phi = 0$ implies $\Phi = 0$ which means the state is plastic
- if $\Phi < 0$, then $\dot{\lambda}\Phi = 0$ implies $\dot{\lambda} = 0$ and from (3.2c) we get that the state is elastic.

Since $\Phi = 0$, $\dot{\lambda} > 0$ when plastic loading persists, the third equation in (3.3) leads to the so-called plastic consistency condition:

$$\dot{\lambda}\dot{\Phi} = 0 \tag{3.4}$$

3.3 The J_2 formulation for fiber stress state

3.3.1 Mapping on the constrained stress space

We begin by defining the admissible stress space for a planar beam fiber, $\mathcal{S}$:

$$\mathcal{S} = \{\vec{\boldsymbol{\sigma}} \in \mathbb{R}^6 \mid \sigma_{22} = \sigma_{33} = \sigma 23 = \sigma_{13} = 0\}$$

The von Mises yield criterion is stated as follows:

$$\Phi(J_2, e^{pl}) = \sqrt{3J_2} - q(e^{pl}) \leq 0 \tag{3.5}$$

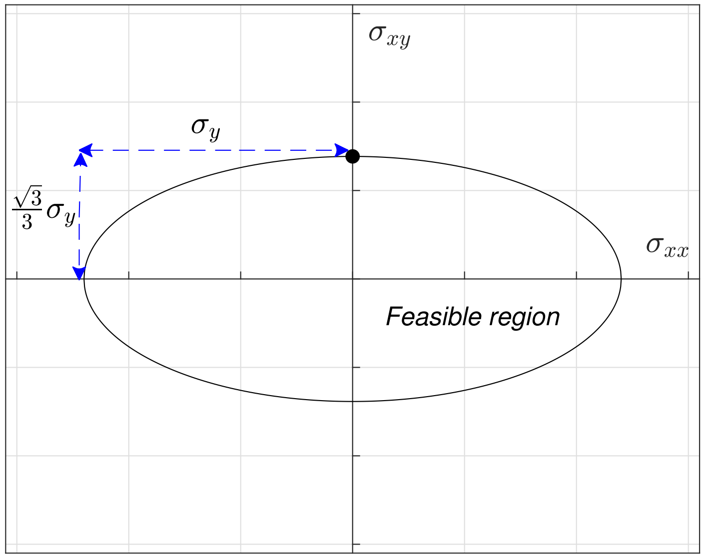

Fig. 3.1. Feasible space and yield locus for the J_2 model. At the boundary of the ellipse, $\sqrt{3J_2} = q$.

where J_2 is the second invariant of the deviatoric stress tensor:

$$J_2 = \frac{1}{2}\boldsymbol{\sigma}^d : \boldsymbol{\sigma}^d \tag{3.6}$$

The deviatoric part of any tensor is given by $(\ )^d = (\ ) - \frac{1}{3}\mathbf{I} \cdot \mathrm{trace}[(\ )]$, with $\mathbf{I}$ being the identity tensor and symbol ¡:¿ designates the contraction operator: $\boldsymbol{\sigma}^d : \boldsymbol{\sigma}^d = \sum_{i,j} \sigma^d_{ij}\sigma^d_{ij}$.

In the von Mises J_2 framework, the hydrostatic pressure cannot cause plastic flow. In other words, plastic deformation is due to the deviatoric components of the stress tensor and volume changes are caused only by elastic deformations. This implies that trace[$\boldsymbol{\epsilon}^{pl}$]$= 0$ which, coupled with Eq. (3.2d), also leads to trace[$\boldsymbol{\alpha}^{pl}$]$= 0$. This means that the back stress tensor in Eq. (3.2d) deviatoric.

In active stress space $\mathcal{S}$ the yield function is $\Phi = \sqrt{\sigma_{11}^2 + 3\sigma_{12}^2} - q$ describes an ellipse, shown in 3.1, with semi-major and semi-minor axes σ_y, $\sqrt{3}/3\sigma_y$, respectively.

When kinematic hardening is included, we introduce the effective stress tensor and its deviatoric part in order to facilitate notational simplicity:

$$\boldsymbol{\zeta} = \boldsymbol{\sigma} - \boldsymbol{\alpha}, \qquad \boldsymbol{\zeta}^d = \boldsymbol{\sigma}^d - \boldsymbol{\alpha}^d \tag{3.7}$$

We now define the following vectors associated with the active tensor components that explicitly enter subsequent derivations:

$$\vec{\boldsymbol{\alpha}}_f = \begin{bmatrix} \alpha_{11} \\ \alpha_{12} \end{bmatrix}, \quad \vec{\boldsymbol{\alpha}}_f^d = \begin{bmatrix} \alpha_{11}^d \\ \alpha_{12}^d \end{bmatrix}, \quad \vec{\boldsymbol{\epsilon}}_f^{pl} = \begin{bmatrix} \epsilon_{11}^{pl} \\ \gamma_{12}^{pl} \end{bmatrix},$$
$$\vec{\boldsymbol{\sigma}}_f^d = \begin{bmatrix} \sigma_{11}^d \\ \sigma_{12}^d \end{bmatrix}, \quad \vec{\boldsymbol{\zeta}}_f = \begin{bmatrix} \zeta_{11} \\ \zeta_{12} \end{bmatrix}, \quad \vec{\boldsymbol{\zeta}}_f^d = \begin{bmatrix} \zeta_{11}^d \\ \zeta_{12}^d \end{bmatrix}$$

The vector representation of (3.6) in terms of the effective stress is:

$$J_2 = \frac{1}{2}(\vec{\boldsymbol{\zeta}}^d)^T \mathbf{J} \vec{\boldsymbol{\zeta}}^d \tag{3.8}$$

where matrix $\mathbf{J} = \text{diag}[1, 1, 1, 2, 2, 2]$ is introduced to account for the symmetry of $\boldsymbol{\zeta}^d$.

We now seek a mapping from the deviatoric stress space onto the fiber stress space S of the deviatoric effective stress vector $\vec{\boldsymbol{\zeta}}^d$ that preserves the inner product and, thus, the second deviatoric invariant J_2. The non-zero components of $\vec{\boldsymbol{\zeta}}^d$ are $\zeta_{11}^d,\ \zeta_{22}^d,\ \zeta_{33}^d,\ \zeta_{12}^d,\ \zeta_{21}^d$ and thus we can establish the following mappings between the active components of $\vec{\boldsymbol{\zeta}}^d$ and $\vec{\boldsymbol{\zeta}}_f$:

$$\vec{\boldsymbol{\zeta}}^d = \mathbf{Q}\vec{\boldsymbol{\zeta}}_f, \qquad \vec{\boldsymbol{\zeta}}_f^d = \mathbf{S}\vec{\boldsymbol{\zeta}}_f \tag{3.9}$$

where the mapping matrices above are given by:

$$\mathbf{Q} = \begin{bmatrix} \frac{2}{3} & -\frac{1}{3} & -\frac{1}{3} & 0 & 0 & 0 \\ 0 & 0 & 0 & 1 & 0 & 0 \end{bmatrix}^T, \qquad \mathbf{S} = \begin{bmatrix} \frac{2}{3} & 0 \\ 0 & 1 \end{bmatrix} \tag{3.10}$$

We can now express J_2 purely in terms of $\vec{\boldsymbol{\zeta}}_f$:

$$J_2 = \frac{1}{2}(\vec{\boldsymbol{\zeta}}^d)^T \mathbf{J} \vec{\boldsymbol{\zeta}}^d = \frac{1}{2}\vec{\boldsymbol{\zeta}}_f^T \mathbf{Q}^T \mathbf{J} \mathbf{Q} \vec{\boldsymbol{\zeta}}_f = \frac{1}{2}\vec{\boldsymbol{\zeta}}_f^T \mathbf{V} \vec{\boldsymbol{\zeta}}_f = \frac{1}{2}\|\vec{\boldsymbol{\zeta}}_f\|_{\boldsymbol{V}}^2 \tag{3.11}$$

where $\mathbf{V} = \mathrm{diag}[\frac{2}{3}, 2]$ and the notation used for the inner product induced by matrix $\mathbf{A}$ between vectors $\vec{\boldsymbol{w}}$, $\vec{\boldsymbol{v}}$ is $(\vec{\boldsymbol{w}}, \vec{\boldsymbol{v}})_{\boldsymbol{A}} = \vec{\boldsymbol{w}}^T \mathbf{A} \vec{\boldsymbol{v}}$, which leads to the notation adopted in Eq. (3.11).

With these derivations at hand, system (3.2) can be recast in the constrained fiber stress state as follows:

$$\dot{\vec{\boldsymbol{\epsilon}}}_f = \dot{\vec{\boldsymbol{\epsilon}}}_f^{el} + \dot{\vec{\boldsymbol{\epsilon}}}_f^{pl} \qquad \text{(Strain decomposition)} \tag{3.12a}$$

$$\dot{\vec{\boldsymbol{\sigma}}}_f = \mathbf{C}^{el}\left[\dot{\vec{\boldsymbol{\epsilon}}}_f - \dot{\vec{\boldsymbol{\epsilon}}}_f^{pl}\right] \qquad \text{(Elastic constitutive law)} \tag{3.12b}$$

$$\dot{\vec{\boldsymbol{\epsilon}}}_f^{pl} = \dot{\lambda}\vec{\boldsymbol{n}} \qquad \text{(Flow rule)} \tag{3.12c}$$

$$\dot{\vec{\boldsymbol{\alpha}}}_f = \dot{\lambda} H_{kin} \mathbf{V}^{-1} \vec{\boldsymbol{n}} \qquad \text{(Kinematic hardening law)} \tag{3.12d}$$

$$\dot{q}_f = \dot{\lambda}\frac{\partial q_f}{\partial e_f^{pl}} \qquad \text{(Isotropic hardening law)} \tag{3.12e}$$

$$\Phi(\vec{\boldsymbol{\zeta}}_f, e^{pl}) = \sqrt{\frac{3}{2}}\|\vec{\boldsymbol{\zeta}}_f\|_{\boldsymbol{V}} - q_f(e_f^{pl}) \leq 0 \qquad \text{(Yield criterion)} \tag{3.12f}$$

Vector $\vec{\boldsymbol{n}}$ is expressed as follows:

$$\vec{\boldsymbol{n}} = \frac{\partial \Phi}{\partial \boldsymbol{\sigma}_f} = -\frac{\partial \Phi}{\partial \boldsymbol{\alpha}_f} = \sqrt{\frac{3}{2}}\frac{\mathbf{V}\vec{\boldsymbol{\zeta}}_f}{\|\vec{\boldsymbol{\zeta}}_f\|_{\boldsymbol{V}}} \tag{3.13}$$

Equations (3.2e), (3.2f) remain the same in the current system. In addition, note that for the J_2 model, the left-hand side of eq. (3.2d) is a deviatoric tensor whereas in (3.12d) it has been mapped to fiber stress space $\mathcal{S}$.

3.3.2 Continuous tangent modulus

The continuous elastoplastic modulus $\mathbf{C}^{ep}$ is found by enforcing the plastic consistency condition (3.4) during a plastic step:

$$\vec{\boldsymbol{n}}^T \dot{\vec{\boldsymbol{\zeta}}}_f - \dot{\lambda} \frac{\partial q_f}{\partial e_f^{pl}} = 0 \tag{3.14}$$

The rate form for the effective stress is given by combining Eqs. (3.12b), (3.12d) with $\dot{\vec{\boldsymbol{\zeta}}}_f = \dot{\vec{\boldsymbol{\sigma}}}_f - \dot{\vec{\boldsymbol{\alpha}}}_f$:

$$\dot{\vec{\boldsymbol{\zeta}}}_f = \mathbf{C}^{el} \dot{\epsilon}_f - \dot{\lambda} \mathbf{Z} \vec{\boldsymbol{n}} \tag{3.15}$$

where $\mathbf{Z} = \mathbf{C}^{el} + H_{kin} \mathbf{V}^{-1}$. Substituting (3.15) into (3.14) and solving for $\dot{\lambda}$ we get:

$$\dot{\lambda} = \frac{\vec{\boldsymbol{n}}^T \mathbf{C}^{el} \dot{\vec{\boldsymbol{\epsilon}}}_f}{\vec{\boldsymbol{n}}^T \mathbf{Z} \vec{\boldsymbol{n}} + \frac{\partial q_f}{\partial e_f^{pl}}} \tag{3.16}$$

Finally, by making use of (3.16), (3.12c) and (3.12b), we arrive at the expression for the continuous elastoplastic modulus:

$$\mathbf{C}^{pl} = \mathbf{C}^{el} - \frac{\vec{\boldsymbol{m}} \vec{\boldsymbol{m}}^T}{\vec{\boldsymbol{n}}^T \mathbf{Z} \vec{\boldsymbol{n}} + \frac{\partial q_f}{\partial e_f^{pl}}} \tag{3.17}$$

where $\vec{\boldsymbol{m}} = \mathbf{C}^{el} \vec{\boldsymbol{n}}$.

3.4 Implicit integration of rate equations

We employ the fully implicit backward Euler method to discretize the rate constitutive equations in system (3.12) in the pseudotime interval $[t_n, t_{n+1}]$. We regard the incremental/iterative process as strain driven, in that at the start of increment n, the dependent state variables for each fiber, $S_n = \{\vec{\boldsymbol{\epsilon}}_f, \vec{\boldsymbol{\epsilon}}_f^{pl}, \vec{\boldsymbol{\alpha}}_f, e_f^{pl}\}_n$, are known and stored. We also know the increment in the centerline strain vector $\vec{\boldsymbol{d}}$, $\Delta \vec{\boldsymbol{d}}$. The incremental strain vector for the current fiber is then determined using eq. (2.53b):

$$\Delta\vec{\boldsymbol{\epsilon}}_f = \mathbf{N}_s \Delta\vec{\boldsymbol{q}}$$

Given the incremental strain vector $\Delta\vec{\boldsymbol{\epsilon}}_f$, we need to update the state variables for t_{n+1}: $S_n \rightarrow S_{n+1}$. In what follows we ommit the subscript denoting the vector pertains to the fiber state:

$$S_n \equiv \{\vec{\boldsymbol{\epsilon}}_n, \vec{\boldsymbol{\epsilon}}^{pl}_n, \vec{\boldsymbol{\alpha}}_n, e^{pl}_n\}, \qquad S_{n+1} \equiv \{\vec{\boldsymbol{\epsilon}}_{n+1}, \vec{\boldsymbol{\epsilon}}^{pl}_{n+1}, \vec{\boldsymbol{\alpha}}_{n+1}, e^{pl}_{n+1}\},$$

The update of the fiber total strain vector $\vec{\boldsymbol{\epsilon}}$ is trivial: $\vec{\boldsymbol{\epsilon}}_{n+1} = \vec{\boldsymbol{\epsilon}}_n + \Delta\vec{\boldsymbol{\epsilon}}$. For the remaining state variables the rate system (3.12) is discretized as follows:

$$\vec{\boldsymbol{\sigma}}_{n+1} = \mathbf{C}^{el}\left[\vec{\boldsymbol{\epsilon}}_{n+1} - \vec{\boldsymbol{\epsilon}}^{pl}_{n+1}\right] \tag{3.18a}$$

$$\vec{\boldsymbol{\epsilon}}^{pl}_{n+1} = \vec{\boldsymbol{\epsilon}}^{pl}_n + \dot{\lambda}\vec{\boldsymbol{n}}_{n+1} \tag{3.18b}$$

$$\vec{\boldsymbol{\alpha}}_{n+1} = \vec{\boldsymbol{\alpha}}_n + \lambda H_{kin}\mathbf{V}^{-1}\vec{\boldsymbol{n}}_{n+1} \tag{3.18c}$$

$$q_{n+1} = q_n + \lambda\frac{\partial q_{n+1}}{\partial e^{pl}_{n+1}} \tag{3.18d}$$

$$\Phi(\vec{\boldsymbol{\zeta}}_{n+1}, e^{pl}_{n+1}) = \sqrt{\frac{3}{2}}\|\vec{\boldsymbol{\zeta}}_{n+1}\|_{\boldsymbol{V}} - q_{n+1}(e^{pl}_{n+1}) \leq 0 \tag{3.18e}$$

and

$$\vec{\boldsymbol{\zeta}}_{n+1} = \vec{\boldsymbol{\sigma}}_{n+1} - \vec{\boldsymbol{\alpha}}_{n+1} \tag{3.19}$$

3.4.1 Elastic predictor - Plastic Corrector algorithm

It is convenient to recast system (3.18) purely in terms of stress by utilizing (3.19),(3.18a),(3.18c):

Stress rate system

$$\dot{\vec{\zeta}} = \mathbf{C}^{el}\dot{\vec{\epsilon}} - \dot{\lambda}\mathbf{Z}\vec{n} \qquad (3.20a)$$

$$\dot{q} = \dot{\lambda}\frac{\partial q}{\partial e^{pl}} \qquad (3.20b)$$

Discretized system

$$\vec{\zeta}_{n+1} = \vec{\zeta}_n + \mathbf{C}^{el}\Delta\vec{\epsilon}_{n+1} - \lambda\mathbf{Z}\vec{n}_{n+1} \qquad (3.21a)$$

$$q_{n+1} = q_n + \lambda\frac{\partial q_{n+1}}{\partial e^{pl}_{n+1}} \qquad (3.21b)$$

We need not differentiate between initial and final value for the plastic parameter λ since it is initialized to zero at the beginning of every step: $\lambda_n = 0$. The solution of (3.21) is based on a two-step procedure. The first phase is called trial elastic step, where we assume that the increment $\Delta\vec{\epsilon}$ is elastic and all state variables are updated by setting $\lambda = 0$: $S_n \to S^{TR}_{n+1}$. If the trial stresses satisfy the yield condition $\Phi^{TR}_{n+1} < 0$, then the step was indeed elastic and we can set $S^{TR}_{n+1} \to S_{n+1}$. If the yield criterion is violated, $\Phi^{TR}_{n+1} > 0$, then the step is plastic and we need to apply (plastic) corrections to the state variables so that, upon convergence, we have achieved $\Phi_{n+1} = 0$. This procedure is referred to as Elastic Predictor - Plastic Corrector algorithm and can be traced back to the work of Wilkins[22]. It has enjoyed widespread application in solving problems in elastoplasticity[23, 24, 25, 26, 27, 28] and the basic relations for each step are summarized below.

Elastic Predictor

$$\vec{\zeta}^{TR}_{n+1} = \mathbf{C}^{el}\left[\vec{\epsilon}_{n+1} - \vec{\epsilon}^{pl}_n\right] - \vec{\alpha}_n \qquad (3.22a)$$

$$q^{TR}_{n+1} = q_n \qquad (3.22b)$$

$$\Phi^{TR}_{n+1} = f(\vec{\zeta}^{TR}_{n+1}, q^{TR}_{n+1}) \qquad (3.22c)$$

$$\xrightarrow{\Phi^{TR}_{n+1} > 0}$$

Plastic Corrector

$$\vec{\zeta}_{n+1} = \vec{\zeta}^{TR}_{n+1} - \lambda\mathbf{Z}\vec{n}_{n+1} \qquad (3.23a)$$

$$q_{n+1} = q^{TR}_{n+1} + \lambda\frac{\partial q_{n+1}}{\partial e^{pl}_{n+1}} \qquad (3.23b)$$

$$\Phi_{n+1} = 0 \qquad (3.23c)$$

The Plastic Corrector step is a system of 4 nonlinear algebraic equations with 4 unknowns, $\{\zeta_{11,n+1}, \zeta_{12,n+1}, q_{n+1}, \lambda\}$, and generally a local Newton method is required to determined the unknowns. It should be stressed here that, in multiaxial constitutive algorithms that do not make use of the mapping as developed here, this local process is nested within an upper level Newton procedure that enforces the zero transverse stress condition.

Substituting Eqs. (3.23a),(3.23b) into (3.23c) furnishes a nonlinear scalar equation that needs to be solved for λ. Once λ is computed, then the fiber state can be updated $S^{TR}_{n+1} \rightarrow S_{n+1}$. Refer also to Box 1 for a detailed summary of the plastic updates. Detailed expressions for the local Newton method on $\Phi_{n+1}(\lambda) = 0$ are provided in Appendix C.

3.4.2 Consistent Tangent Modulus

The tangent modulus consistent with the numerical discretization used on system (3.12) is necessary to restore the quadratic rates of convergence for the global Newton method[29]. That is:

$$\mathbf{C}^{pl}_{c} = \frac{\mathrm{d}\vec{\boldsymbol{\sigma}}_{n+1}}{\mathrm{d}\vec{\boldsymbol{\epsilon}}_{n+1}} \tag{3.24}$$

We take the differentials of (3.18a), (3.18c) and (3.18e), using the fact that $\mathrm{d}\vec{\boldsymbol{\zeta}}_{n+1} = \mathrm{d}\vec{\boldsymbol{\sigma}}_{n+1} - \mathrm{d}\vec{\boldsymbol{\alpha}}_{n+1}$ from (3.19) and arrive at the following system:

$$\begin{bmatrix} \mathbf{C}^{el} + \lambda \mathbf{B}_{n+1} & -\lambda \mathbf{B}_{n+1} \\ -\lambda \mathbf{B}_{n+1} & H^{-1}_{kin}\mathbf{V} + \lambda \mathbf{B}_{n+1} \end{bmatrix} \begin{bmatrix} \mathrm{d}\vec{\boldsymbol{\sigma}}_{n+1} \\ \mathrm{d}\vec{\boldsymbol{\alpha}}_{n+1} \end{bmatrix} = \begin{bmatrix} \mathrm{d}\vec{\boldsymbol{\epsilon}}_{n+1} - \mathrm{d}\lambda \vec{\boldsymbol{n}}_{n+1} \\ \mathrm{d}\lambda \vec{\boldsymbol{n}}_{n+1} \end{bmatrix} \tag{3.25a}$$

$$\vec{\boldsymbol{n}}^{T}_{n+1} \left[\mathrm{d}\vec{\boldsymbol{\sigma}}_{n+1} - \mathrm{d}\vec{\boldsymbol{\alpha}}_{n+1} \right] = \mathrm{d}\lambda \frac{\partial q_{n+1}}{\partial e^{pl}_{n+1}} \tag{3.25b}$$

where $\mathbf{B}$ is given as follows:

$$\mathbf{B} = \frac{\partial \vec{\boldsymbol{n}}}{\partial \vec{\boldsymbol{\zeta}}} = \frac{\partial^2 f}{\partial \vec{\boldsymbol{\zeta}}^2} = \frac{1}{\|\vec{\boldsymbol{\zeta}}\|_{\boldsymbol{V}}} \left[\mathbf{V} - \vec{\boldsymbol{n}}\vec{\boldsymbol{n}}^{T} \right] \tag{3.26}$$

Upon solving (3.25a) for $\mathrm{d}\vec{\boldsymbol{\sigma}}_{n+1}$, $\mathrm{d}\vec{\boldsymbol{\alpha}}_{n+1}$ we substitute them into (3.25b) and solve for $\mathrm{d}\lambda$:

$$\mathrm{d}\lambda = \frac{\vec{\boldsymbol{n}}^{T}_{n+1} \left[\boldsymbol{\Xi}_{11} + \boldsymbol{\Xi}^{T}_{12} \right] \mathrm{d}\vec{\boldsymbol{\epsilon}}_{n+1}}{\vec{\boldsymbol{n}}^{T}_{n+1} \mathbf{T} \vec{\boldsymbol{n}}_{n+1} + \frac{\partial q_{n+1}}{\partial e^{pl}_{n+1}}} \tag{3.27}$$

Finally, substituting dλ into (3.18a) furnishes the formula for the consistent tangent modulus:

$$\mathbf{C}_c^{pl} = \mathbf{\Xi}_{11} - \frac{\vec{\boldsymbol{N}}_{n+1}\vec{\boldsymbol{N}}_{n+1}^T}{1+\delta_{n+1}} \tag{3.28}$$

Details regarding all newly defined vectors and matrices involved in the derivation of $\mathbf{C}_c^{pl}$ is given in Appendix D. In Box 1 we have summarised the return mapping algorithnm for a fiber.

3.4.3 Consistent Section Stiffness

Once the stress update on a particular fiber has been carried out, its contribution to the stress resultant vector and the section stiffness are accounted for via a midpoint integration rule along the section height (see Eqs. (2.56), (2.58).

Notice that while in the present formulation $C_{21} = C_{12}$, this will not be the case if a generalized integration rule is used for the rate equations. In such a scenario, if enforcement of the plastic consistency does not correspond to the interior time $t_a \in [t_n, t_{n+1}]$ chosen, that is $\Phi_a = 0$, then the consistenttangent will not be symmetric. For more details on this refer to [30].

Box 1 : Summary of Elastic Predictor - Plastic Corrector algorithm.

- **Start of step - Elastic Predictor**

  - $\vec{\boldsymbol{\epsilon}}^{pl,TR}_{n+1} = \vec{\boldsymbol{\epsilon}}^{pl}_{n}$
  - $e^{pl,TR}_{n+1} = e^{pl}_{n}$
  - $\vec{\boldsymbol{\sigma}}^{TR}_{n+1} = \mathbf{C}^{el}\left[\vec{\boldsymbol{\epsilon}}_{n+1} - \vec{\boldsymbol{\epsilon}}^{pl}_{n}\right]$
  - $q^{TR}_{n+1} = q_n$
  - $\vec{\boldsymbol{\alpha}}^{TR}_{n+1} = \vec{\boldsymbol{\alpha}}_n$
  - $f^{TR}_{n+1} = \Phi(\vec{\boldsymbol{\zeta}}^{TR}_{n+1}, q^{TR}_{n+1})$

- IF $\Phi^{TR}_{n+1} < 0 \rightarrow$ **Elastic Step**

  - $\vec{\boldsymbol{\epsilon}}^{pl}_{n+1} = \vec{\boldsymbol{\epsilon}}^{pl,TR}_{n+1}$
  - $e^{pl}_{n+1} = e^{pl,TR}_{n+1}$
  - $\vec{\boldsymbol{\sigma}}_{n+1} = \vec{\boldsymbol{\sigma}}^{TR}_{n+1}$
  - $q_{n+1} = q^{TR}_{n+1}$
  - $\vec{\boldsymbol{\alpha}}_{n+1} = \vec{\boldsymbol{\alpha}}^{TR}_{n+1}$
  - $\mathbf{C} = \mathbf{C}^{el}$

- ELSE $f^{TR}_{n+1} > 0 \rightarrow$ **Plastic Corrector**

  1. Iteratively solve (3.4.1) for λ: $\lambda^{j+1} = \lambda^{j} - \frac{\Phi^{j}_{n+1}}{(\frac{\mathrm{d}\Phi_{n+1}}{\mathrm{d}\lambda})^{j}}$, with $\lambda^0 = 0$, $\Phi^0_{n+1} = \Phi^{TR}_{n+1}$. Loop termination: $|\Phi^{j+1}_{n+1}| \leq e_{tol}$, where e_{tol} small.

  2. Update state variables:

     - $\vec{\zeta}_{n+1} = [\boldsymbol{\Omega}(\lambda)]\vec{\boldsymbol{\zeta}}^{TR}_{n+1}$
     - $\vec{\boldsymbol{\sigma}}_{n+1} = \vec{\zeta}_{n+1} + \vec{\boldsymbol{\alpha}}_{n+1}$
     - $\vec{\boldsymbol{\epsilon}}^{pl}_{n+1} = \vec{\boldsymbol{\epsilon}}^{pl}_{n} + \lambda\vec{\boldsymbol{n}}_{n+1}$
     - $e^{pl}_{n+1} = e^{pl}_{n} + \lambda$
     - $\vec{\boldsymbol{\alpha}}_{n+1} = \vec{\boldsymbol{\alpha}}_n + \lambda H_{kin}\mathbf{V}^{-1}\vec{\boldsymbol{n}}_{n+1}$
     - $q_{n+1} = q_n + \lambda\dfrac{\partial q_{n+1}}{\partial e^{pl}_{n+1}}$

  3. Get consistent tangent modulus

$$\mathbf{C} = \mathbf{C}^{pl}_{c} = \boldsymbol{\Xi}_{11} - \frac{\vec{\boldsymbol{N}}_{n+1}\vec{\boldsymbol{N}}^{T}_{n+1}}{1 + \delta_{n+1}}$$

See Appendix C for $[\boldsymbol{\Omega}(\lambda)]$.

CHAPTER 4

DISCUSSION

Lorem ipsum dolor sit amet, consectetur adipiscing elit, sed do eiusmod tempor incididunt ut labore et dolore magna aliqua. Ut enim ad minim veniam, quis nostrud exercitation ullamco laboris nisi ut aliquip ex ea commodo consequat. Duis aute irure dolor in reprehenderit in voluptate velit esse cillum dolore eu fugiat nulla pariatur. Excepteur sint occaecat cupidatat non proident, sunt in culpa qui officia deserunt mollit anim id est laborum..

CHAPTER 5

CONCLUSION

Lorem ipsum dolor sit amet, consectetur adipiscing elit, sed do eiusmod tempor incididunt ut labore et dolore magna aliqua. Ut enim ad minim veniam, quis nostrud exercitation ullamco laboris nisi ut aliquip ex ea commodo consequat. Duis aute irure dolor in reprehenderit in voluptate velit esse cillum dolore eu fugiat nulla pariatur. Excepteur sint occaecat cupidatat non proident, sunt in culpa qui officia deserunt mollit anim id est laborum.

Appendices

APPENDIX A

Explicit expressions of the formulation are provided in this Appendix. We note that operations involving the symbol ∇ map scalars to vectors and vectors to matrices. For example, if $f : \mathbb{R}^p \to \mathbb{R}$ and $\vec{\boldsymbol{v}} : \mathbb{R}^p \to \mathbb{R}^q$, then $\nabla f : \mathbb{R}^p \to \mathbb{R}^p$ and $\nabla \vec{\boldsymbol{v}} : \mathbb{R}^p \to \mathbb{R}^{p\times q}$.

The Lagrangian function is used here, as presented in Eq. (2.30):

$$\mathcal{L}(\vec{\boldsymbol{y}}, \vec{\boldsymbol{d}}_g, \vec{\boldsymbol{\lambda}}) = U - W + \vec{\boldsymbol{\lambda}}^T \vec{\boldsymbol{h}}_g \tag{A.1}$$

where it is also reminded that $\vec{\boldsymbol{y}} = \begin{bmatrix} \vec{\boldsymbol{y}}_1^T & \vec{\boldsymbol{y}}_2^T & \cdots & \vec{\boldsymbol{y}}_m^T \end{bmatrix}^T$, $\vec{\boldsymbol{y}}_i = \begin{bmatrix} \vec{\boldsymbol{q}}_i & \phi_i \end{bmatrix}^T$ and $\vec{\boldsymbol{q}}_i = \begin{bmatrix} \epsilon_i & \gamma_i & \kappa_i \end{bmatrix}^T$. The number m designates the total number of integration points in the structure.

A.0.1 Gradient of strain energy

The gradient of U is expressed as:

$$\nabla U = \begin{bmatrix} \nabla_{\mathbf{y}} U \\ \nabla_{\mathbf{d}_g} U \\ \nabla_{\lambda} U \end{bmatrix}$$

The gradient with respect to the strain vector $\vec{\boldsymbol{y}}$ gives the stress resultants at all cross-sections and has the following form for a particular cross-section i:

$$\nabla_{\mathbf{y}_i} U = \begin{bmatrix} w_i N_i \\ w_i V_i \\ w_i M_i \\ 0 \end{bmatrix} = w_i \begin{bmatrix} \vec{\boldsymbol{F}}_{sec}^{(i)} \\ 0 \end{bmatrix} \tag{A.2}$$

it is usually computed by numerical integration of Eqs. (2.55) over the cross-section height. In the case of elastic analysis, the above vector can be computed explicitly for each cross-section, since then $\vec{\boldsymbol{F}}_{sec}^{(i)} = \begin{bmatrix} EA\epsilon_i & k_s GA\gamma_i & EI\kappa_i \end{bmatrix}^T$.

The gradients of U with respect to both $\vec{\boldsymbol{d}}_g$ and $\vec{\boldsymbol{\lambda}}$ provide zero vectors:

$$\nabla_{\mathbf{d}_g} U = \vec{\mathbf{0}} \in \mathbb{R}^{3N} \quad \text{and} \quad \nabla_{\lambda} U = \vec{\mathbf{0}} \in \mathbb{R}^{s}$$

where $s = m + 3n_{el}$, n_{el} being the number of elements. Finally, we then get:

$$\nabla U = \begin{bmatrix} \nabla_{\mathbf{y}} U \\ \vec{\mathbf{0}} \\ \vec{\mathbf{0}} \end{bmatrix} \tag{A.3}$$

A.0.2 Gradient of constraints

We restate the constraints equations from Eqs. (2.32a)-(2.32b):

$$\vec{\boldsymbol{h}}_g = \begin{bmatrix} \vec{\boldsymbol{h}}_g^A \\ \vec{\boldsymbol{h}}_g^B \end{bmatrix} = \begin{bmatrix} \mathbf{V}_1 \vec{\boldsymbol{d}}_g - \boldsymbol{\Lambda}^T \left[\sum_{i=1}^{n} w_i \mathbf{R}_i (\vec{\boldsymbol{q}}_i + \vec{\boldsymbol{E}}_1) - \ell \vec{\boldsymbol{E}}_1 \right] \\ \vec{\boldsymbol{\phi}} - \mathbf{V}_2 \vec{\boldsymbol{d}}_g - \mathbf{T} \vec{\boldsymbol{\kappa}} \end{bmatrix}$$

For notational simplicity, we assume here only one element in the derivations that follow. When more elements are used, their corresponding constraint vectors are stacked in vector form as $\vec{\boldsymbol{h}} = \begin{bmatrix} \vec{\boldsymbol{h}}_g^{1\,T} & \vec{\boldsymbol{h}}_g^{2\,T} & \dots & \vec{\boldsymbol{h}}_g^{n_{el}\,T} \end{bmatrix}^T$. The gradient with respect to the strain vector

$\vec{\boldsymbol{y}}_i$ at a particular cross-section is given by:

$$\nabla_{\mathbf{y}_i}\vec{\boldsymbol{h}}_g^A = \begin{bmatrix}\nabla_{\mathbf{q}_i}\vec{\boldsymbol{h}}_g^A & \dfrac{d\vec{\boldsymbol{h}}_g^A}{d\phi_i}\end{bmatrix} = -w_i\mathbf{\Lambda}^T\begin{bmatrix}\mathbf{R}_i & \mathbf{R}_i\mathbf{X}[\vec{\boldsymbol{q}}_i + \vec{\boldsymbol{E}}_1]\end{bmatrix}$$

where:

$$\frac{d\mathbf{R}_i}{d\phi_i} = \mathbf{R}_i\mathbf{X} \quad \text{and} \quad \mathbf{X} = \begin{bmatrix}0 & -1 & 0\\ 1 & 0 & 0\\ 0 & 0 & 0\end{bmatrix}$$

The gradient of $\vec{\boldsymbol{h}}_g^B$ with respect to strain vector $\vec{\boldsymbol{y}}_i$, is:

$$\nabla_{\mathbf{y}_i}\vec{\boldsymbol{h}}_g^B = \begin{bmatrix}\nabla_{\mathbf{q}_i}\vec{\boldsymbol{h}}_g^B & \dfrac{d\vec{\boldsymbol{h}}_g^B}{d\phi_i}\end{bmatrix} = \begin{bmatrix}\vec{\mathbf{0}} & \vec{\mathbf{0}} & -\mathbf{T}\hat{\mathbf{E}}_i & \hat{\mathbf{E}}_i\end{bmatrix}$$

where $\hat{\mathbf{E}}_i \in \mathbb{R}^n$ is a unit vector with the i-th component equal to one. Collectively, we have:

$$\nabla_{\mathbf{y}_i}\vec{\boldsymbol{h}}_g = \begin{bmatrix}-w_i\mathbf{\Lambda}^T\mathbf{R}_i & -w_i\mathbf{\Lambda}^T\mathbf{R}_i\mathbf{X}[\vec{\boldsymbol{q}}_i + \vec{\boldsymbol{E}}_1]\\ [\vec{\mathbf{0}} \quad \vec{\mathbf{0}} \quad -\mathbf{T}\hat{\mathbf{E}}_i] & \hat{\mathbf{E}}_i\end{bmatrix} \tag{A.4}$$

The gradient with respect to the displacement vector is derived in a straightforward manner by simple derivations:

$$\nabla_{\mathbf{d}_g}\vec{\boldsymbol{h}}_g = \begin{bmatrix}\mathbf{V}_1\\ -\mathbf{V}_2\end{bmatrix} \tag{A.5}$$

$$\mathbf{V}_1 = \begin{bmatrix} -\mathbf{I} & \mathbf{I} \end{bmatrix} \quad , \quad \mathbf{V}_2 = \begin{bmatrix} \vec{\mathbf{0}} & \vec{\mathbf{0}} & \vec{\mathbf{1}} & \vec{\mathbf{0}} & \vec{\mathbf{0}} & \vec{\mathbf{0}} \end{bmatrix}$$

$$\mathbf{I} = \begin{bmatrix} 1 & 0 & 0 \\ 0 & 1 & 0 \\ 0 & 0 & 1 \end{bmatrix} \quad , \quad \vec{\mathbf{0}}, \vec{\mathbf{1}} \in \mathbb{R}^n, \quad \vec{\mathbf{0}} = \begin{bmatrix} 0 & \cdots & 0 \end{bmatrix}^T, \quad \vec{\mathbf{1}} = \begin{bmatrix} 1 & \cdots & 1 \end{bmatrix}^T$$

Finally, the gradient with respect to the vector $\vec{\boldsymbol{\lambda}}$ gives a zero matrix:

$$\nabla_\lambda \vec{\boldsymbol{h}}_g = \mathbf{0} \in \mathbb{R}^{(n+3)\times(n+3)} \tag{A.6}$$

The total constraints gradient is then expressed in block matrix form as:

$$\nabla \vec{\boldsymbol{h}}_g = \begin{bmatrix} \nabla_{\mathbf{y}_1} \vec{\boldsymbol{h}}_g & \nabla_{\mathbf{y}_2} \vec{\boldsymbol{h}}_g & \cdots & \nabla_{\mathbf{y}_n} \vec{\boldsymbol{h}}_g & \nabla_{\mathbf{d}_g} \vec{\boldsymbol{h}}_g & \nabla_\lambda \vec{\boldsymbol{h}}_g \end{bmatrix}$$

Note that in the case of small displacements, only the expression $\nabla_{\mathbf{y}_i} \vec{\boldsymbol{h}}_g^A$ has to be modified, so that the strain-displacement relations reduce to the classical linear Timoshenko theory:

$$\nabla_{\mathbf{y}_i} \vec{\boldsymbol{h}}_g^A = -w_i \boldsymbol{\Lambda}^T \begin{bmatrix} 1 & -\phi_i & 0 & -\gamma_i \\ 0 & 1 & 0 & 1 \\ 0 & 0 & 1 & 0 \end{bmatrix}$$

with the vector of constraints $\vec{\boldsymbol{h}}_g^A$ being:

$$\vec{\boldsymbol{h}}_g^A = \mathbf{V}_1 \vec{\boldsymbol{d}}_g - \boldsymbol{\Lambda}^T \left[\sum_{i=1}^{n} w_i [\hat{\mathbf{R}}_i (\vec{\boldsymbol{q}}_i + \vec{\boldsymbol{E}}_1) - \vec{\boldsymbol{g}}_i] - \ell \vec{\boldsymbol{E}}_1 \right] \tag{A.7}$$

where:

$$\hat{\mathbf{R}}_i = \begin{bmatrix} 1 & -\phi_i & 0 \\ \phi_i & 1 & 0 \\ 0 & 0 & 1 \end{bmatrix}, \quad \vec{\boldsymbol{g}}_i = \begin{bmatrix} 0 \\ \epsilon_i \phi_i \\ 0 \end{bmatrix}$$

The vector $\vec{\boldsymbol{g}}_i$ is added in order to eliminate the second order term $\epsilon_i \phi_i$ arising from the imposition of the small displacement assumption $\sin \phi_i \approx \phi_i$, $\cos \phi_i \approx 1$ in Eq. (2.32a).

A.0.3 Gradient of the potential energy

The potential energy due to external loads $\vec{\boldsymbol{P}}$ is:

$$W = \sum_{j=1}^{N} \vec{\boldsymbol{P}}_j^T \vec{\boldsymbol{d}}_{g,j} = \vec{\boldsymbol{d}}_g^T \vec{\boldsymbol{P}}$$

The gradient of the potential energy is, again, straightforward in its derivation as it only depends on the displacement vector:

$$\nabla W = \begin{bmatrix} \nabla_{\mathbf{y}} W \\ \nabla_{\mathbf{d}_g} W \\ \nabla_{\lambda} W \end{bmatrix}$$

with $\nabla_{\mathbf{y}} W = \vec{\mathbf{0}} \in \mathbb{R}^m$, $\nabla_{\mathbf{d}_g} W = \vec{\boldsymbol{P}}$ and $\nabla_{\lambda} W = \vec{\mathbf{0}} \in \mathbb{R}^{n+3}$ for one element. Thus, we have:

$$\nabla W = \begin{bmatrix} \vec{\mathbf{0}} \\ \vec{\boldsymbol{P}} \\ \vec{\mathbf{0}} \end{bmatrix} \tag{A.8}$$

A.0.4 Gradient of the Lagrangian

We substitute in Eqs. (2.35) the explicit expressions derived here in the Appendix:

$$\nabla_{\mathbf{y}_i}\mathcal{L} = w_i \begin{bmatrix} \vec{\boldsymbol{F}}_{sec}^{(i)} \\ 0 \end{bmatrix} + \begin{bmatrix} -w_i \boldsymbol{\Lambda}^T \mathbf{R}_i & -w_i \boldsymbol{\Lambda}^T \mathbf{R}_i \mathbf{X}[\vec{\boldsymbol{q}}_i + \vec{\boldsymbol{E}}_1] \\ [\vec{\mathbf{0}} \quad \vec{\mathbf{0}} \quad -\mathbf{T}\hat{\mathbf{E}}_i] & \hat{\mathbf{E}}_i \end{bmatrix}^T \vec{\boldsymbol{\lambda}} \tag{A.9}$$

$$\nabla_{\mathbf{d}_g}\mathcal{L} = -\begin{bmatrix} \vec{\mathbf{0}} \\ \vec{\boldsymbol{P}} \\ \vec{\mathbf{0}} \end{bmatrix} + \begin{bmatrix} \mathbf{V}_1 \\ -\mathbf{V}_2 \end{bmatrix}^T \vec{\boldsymbol{\lambda}} \tag{A.10}$$

$$\nabla_\lambda \mathcal{L} = \vec{\boldsymbol{h}}_g \tag{A.11}$$

APPENDIX B

The Hessian form in Eq. (2.36), is restated here:

$$\mathbf{H} = \begin{bmatrix} \nabla^2_{\mathbf{yy}}\mathcal{L} & \mathbf{0} & \nabla_{\mathbf{y}}\vec{\boldsymbol{h}}_g^T \\ \mathbf{0} & \mathbf{0} & \nabla_{\mathbf{d_g}}\vec{\boldsymbol{h}}_g^T \\ \nabla_{\mathbf{y}}\vec{\boldsymbol{h}}_g & \nabla_{\mathbf{d_g}}\vec{\boldsymbol{h}}_g & \mathbf{0} \end{bmatrix}$$

The gradients of $\vec{\boldsymbol{h}}_g$ have been derived in the previous section. Thus, for the complete specification of the second order information we need only to determine the second derivative matrix with respect to the strain vector $\vec{\boldsymbol{y}}$. Since different integration points are independent of one another, then it is clear that $\nabla^2_{\mathbf{y}_i\mathbf{y}_j}\mathcal{L} = \mathbf{0}$ for $i \neq j$. Therefore, the matrix $\nabla^2_{\mathbf{yy}}\mathcal{L}$ has a block diagonal form:

$$\nabla^2_{\mathbf{yy}}\mathcal{L} = \begin{bmatrix} \nabla^2_{\mathbf{y}_i\mathbf{y}_i}\mathcal{L} & \mathbf{0} & \cdots & \mathbf{0} \\ \mathbf{0} & \nabla^2_{\mathbf{y}_i\mathbf{y}_i}\mathcal{L} & \cdots & \mathbf{0} \\ \vdots & \ddots & & \vdots \\ \mathbf{0} & \cdots & \mathbf{0} & \nabla^2_{\mathbf{y}_m\mathbf{y}_m}\mathcal{L} \end{bmatrix}$$

and making use of Eq. (2.60) gives:

$$\nabla^2_{\mathbf{y}_i\mathbf{y}_i}\mathcal{L} = \nabla^2_{\mathbf{y}_i\mathbf{y}_i}U + \nabla_{\mathbf{y}_i}([\nabla_{\mathbf{y}_i}\vec{\boldsymbol{h}}_g]^T\vec{\boldsymbol{\lambda}}) \tag{B.1}$$

As already seen, the second derivative matrix of the strain energy yields the generalized section stiffness of cross-section i:

$$\nabla^2_{\mathbf{y}_i\mathbf{y}_i} U = w_i \begin{bmatrix} \mathbf{k}^{(i)}_{sec} & \mathbf{0} \\ \mathbf{0} & 0 \end{bmatrix}$$

where $\mathbf{k}^{(i)}_{sec}$ is given by Eq. (2.58) after numerical integration of the cross-section. We only now need to derive the explicit form for the second term of the right hand side in Eq. (B.1). To this end, we separate the Lagrange multiplier vector into two parts, which correspond to vectors $\vec{\boldsymbol{h}}^A_h$ and $\vec{\boldsymbol{h}}^B_h$ respectively:

$$\vec{\boldsymbol{\lambda}} = \begin{bmatrix} \vec{\boldsymbol{\lambda}}^A \\ \vec{\boldsymbol{\lambda}}^B \end{bmatrix}$$

Eq. (A.9) can be now restated as:

$$\nabla_{\mathbf{y}_i}\mathcal{L} = w_i \begin{bmatrix} \vec{\boldsymbol{F}}^{(i)}_{sec} \\ 0 \end{bmatrix} - w_i \begin{bmatrix} \mathbf{R}^T_i \boldsymbol{\Lambda} \\ [\vec{\boldsymbol{q}}_i + \vec{\boldsymbol{E}}_1]^T \mathbf{X}^T \mathbf{R}_i \boldsymbol{\Lambda} \end{bmatrix} \vec{\boldsymbol{\lambda}}^A + \begin{bmatrix} \vec{\mathbf{0}}^T \\ \vec{\mathbf{0}}^T \\ -\hat{\mathbf{E}}^T_i \mathbf{T}^T \\ \hat{\mathbf{E}}^T_i \end{bmatrix} \vec{\boldsymbol{\lambda}}^B \tag{B.2}$$

Noticing that the gradient of $\vec{\boldsymbol{h}}^B_g$ yields components independent of strains, we conclude that the second derivatives of $\mathcal{L}$ will include only the part $\vec{\boldsymbol{\lambda}}^A$, as:

$$\nabla^2_{\mathbf{y}_i\mathbf{y}_i}\mathcal{L} = \nabla^2_{\mathbf{y}_i\mathbf{y}_i} U + \mathbf{Z}_i \tag{B.3}$$

where:

$$\mathbf{Z}_i = \begin{bmatrix} \mathbf{0}_{(3\times3)} & \vec{\boldsymbol{t}}_i \\ \vec{\boldsymbol{t}}^T_i & \vec{\boldsymbol{t}}^T_i \mathbf{X}[\vec{\boldsymbol{q}}_i + \vec{\boldsymbol{E}}_1] \end{bmatrix} \quad \text{and} \quad \vec{\boldsymbol{t}}_i = -w_i \mathbf{X}^T \mathbf{R}^T_i \boldsymbol{\Lambda} \vec{\boldsymbol{\lambda}}^A$$

and the second derivative matrix of the Lagrangian is now fully determined.

APPENDIX C

First, we express the effective stress vector $\vec{\boldsymbol{\zeta}}_{n+1}$ purely in terms λ, using eq. (3.23a) and the fact that $\vec{\boldsymbol{n}} = \sqrt{\frac{3}{2}}\frac{\mathbf{V}\vec{\boldsymbol{\zeta}}}{\|\vec{\boldsymbol{\zeta}}\|_{\boldsymbol{V}}}$:

$$\left[\mathbf{I} + \frac{\lambda\sqrt{\frac{3}{2}}}{\|\vec{\boldsymbol{\zeta}}_{n+1}\|_{\boldsymbol{V}}}\left[\mathbf{C}^{el}\mathbf{V} + H_{kin}\mathbf{I}\right]\right]\vec{\boldsymbol{\zeta}}_{n+1} = \vec{\boldsymbol{\zeta}}^{TR}_{n+1} \tag{C.1}$$

In the first phase of a plastic step we assume that no plastic flow occurs (Elsatic Prediction), therefore, for the purposes of the iterative strategy we can consider the following identity:

$$f_{n+1} = 0 \rightarrow \|\vec{\boldsymbol{\zeta}}_{n+1}\|_{\boldsymbol{V}} = q_n + \lambda\sqrt{\frac{2}{3}}\frac{\partial q_n}{\partial e^{pl}_n} \tag{C.2}$$

In the case of linear isotropic hardening, eq. (C.2) is exact since $\frac{\partial q}{\partial e^{pl}} = H_{iso}$. Otherwise the isotropic modulus used in the context of the fully implicit integration is replaced with the one at the previous step for the purposes of the iterative strategy and only for that. This technique is done so that $\vec{\boldsymbol{\zeta}}_{n+1}$ is recast only in terms of λ. Substituting (C.2) into (C.1) and solving for $\vec{\boldsymbol{\zeta}}_{n+1}$ we get:

$$\vec{\boldsymbol{\zeta}}_{n+1} = \boldsymbol{\Omega}\vec{\boldsymbol{\zeta}}^{TR}_{n+1} \tag{C.3}$$

Let $a_1 = E + \frac{3}{2}H_{kin} + \frac{\partial q_n}{\partial e^{pl}_n}$ and $a_2 = 3G + \frac{3}{2}H_{kin} + \frac{\partial q_n}{\partial e^{pl}_n}$. Then:

$$\boldsymbol{\Omega} = \left[\mathbf{I} + \frac{\lambda\sqrt{\frac{3}{2}}}{q_n + \lambda\sqrt{\frac{2}{3}}\frac{\partial q_n}{\partial e^{pl}_n}}\left[\mathbf{C}^{el}\mathbf{V} + H_{kin}\mathbf{I}\right]\right]^{-1} = \mathrm{diag}\left(\frac{q_n + \lambda\frac{\partial q_n}{\partial e^{pl}_n}}{q_n + \lambda a_1}, \frac{q_n + \lambda\frac{\partial q_n}{\partial e^{pl}_n}}{q_n + \lambda a_2}\right) \tag{C.4}$$

Substitution of (C.3) into $f(\vec{\boldsymbol{\zeta}}_{n+1}, q_{n+1}) \equiv f_{n+1} = 0$ yields the scalar equation to be solved iteratively for λ:

$$f_{n+1} = \sqrt{\frac{3}{2}}\sqrt{(\vec{\boldsymbol{\zeta}}^{TR}_{n+1})^T \boldsymbol{\Omega} \mathbf{V} \boldsymbol{\Omega} \vec{\boldsymbol{\zeta}}^{TR}_{n+1}} - q_{n+1} = 0 \tag{C.5}$$

The derivative of f_{n+1} with respect to λ involves finding the derivative of the diagonal matrix $\boldsymbol{\Omega}$ and a chain rule with respect to q_{n+1}. It can be found that the derivative is:

$$\frac{\mathrm{d}f_{n+1}}{\mathrm{d}\lambda} = -\frac{1}{q_n}\left[\frac{n_{11}\zeta^{TR}_{11}(E + \frac{3}{2}H_{kin})}{(1 + \frac{\lambda a_1}{q_n})^2} + \frac{n_{12}\zeta^{TR}_{12}(3G + \frac{3}{2}H_{kin})}{(1 + \frac{\lambda a_2}{q_n})^2}\right] - (1 + \lambda)\frac{\partial q_{n+1}}{\partial e^{pl}_{n+1}} \tag{C.6}$$

APPENDIX D

For the inversion of the block matrix (3.25a) we perform block elimination considering $\mathbf{A} = \mathbf{C}^{el} + \lambda\mathbf{B} - \lambda^2\mathbf{B}_{n+1}\Big[H_{kin}\mathbf{V} + \lambda\mathbf{B}_{n+1}\Big]^{-1}\mathbf{B}_{n1+}$ as the Schur complement. Notice that while the matrix $\lambda\mathbf{B}_{n+1}$ is not invertible, the diagonal ones are. Omitting the subscript refering to the step, inversion of system (3.25a) yields:

$$\begin{bmatrix} \mathrm{d}\vec{\boldsymbol{\sigma}} \\ \mathrm{d}\vec{\boldsymbol{\alpha}} \end{bmatrix} = \begin{bmatrix} [\boldsymbol{\Xi}]_{11} & [\boldsymbol{\Xi}]_{12} \\ [\boldsymbol{\Xi}]_{21} & [\boldsymbol{\Xi}]_{22} \end{bmatrix} \begin{bmatrix} \mathrm{d}\vec{\boldsymbol{\epsilon}} - \mathrm{d}\lambda\vec{\boldsymbol{n}} \\ \mathrm{d}\lambda\vec{\boldsymbol{n}} \end{bmatrix} \tag{D.1}$$

and define $\boldsymbol{\Gamma} = \lambda\mathbf{B}\Big(H_{kin}^{-1}\mathbf{V} + \lambda\mathbf{B}\Big)^{-1}$. Then, for the block matrices $[\boldsymbol{\Xi}_{ij}]$ we have:

- $[\boldsymbol{\Xi}_{11}] = \mathbf{A}^{-1}$, the inverse of the Schur complement.
- $[\boldsymbol{\Xi}_{12}] = [\boldsymbol{\Xi}_{11}]\boldsymbol{\Gamma}$
- $[\boldsymbol{\Xi}_{21}] = [\boldsymbol{\Xi}_{12}]^T$
- $[\boldsymbol{\Xi}_{22}] = \Big(H_{kin}^{-1}\mathbf{V} + \lambda\mathbf{B}\Big)^{-1} + \boldsymbol{\Gamma}[\boldsymbol{\Xi}_{11}]\boldsymbol{\Gamma}$

where the fact that matrices $\mathbf{B}$ and $\boldsymbol{\Gamma}$ are symmetric was used. The vector $\vec{\boldsymbol{N}}$ in (3.28) is given by:

$$\vec{\boldsymbol{N}} = \frac{\Big[[\boldsymbol{\Xi}_{11}] + [\boldsymbol{\Xi}_{12}]\Big]\vec{\boldsymbol{n}}}{\|\vec{\boldsymbol{n}}\|_{\boldsymbol{T}}} \tag{D.2}$$

with $\mathbf{T} = [\boldsymbol{\Xi}_{11}] + [\boldsymbol{\Xi}_{22}] + [\boldsymbol{\Xi}_{12}] + [\boldsymbol{\Xi}_{21}]$. Finally, parameter δ is defined as:

$$\delta = \frac{\frac{\partial q}{\partial e^{pl}}}{\|\vec{\boldsymbol{n}}\|_{\boldsymbol{T}}^2} \tag{D.3}$$

The calculation can be simplified significantly if second and higher order terms in λ are ignored.

BIBLIOGRAPHY

[1] E. Reissner, "On one-dimensional finite-strain beam theory: The plane problem," Zeitschrift für Angewandte Mathematik und Physik ZAMP, vol. 23, no. 5, pp. 795–804, 1972.

[2] J. Simo, "A finite strain beam formulation. The three-dimensional dynamic problem. Part I," Computer Methods in Applied Mechanics and Engineering, vol. 49, no. 1, pp. 55–70, 1985.

[3] J. Simo and L. Vu-Quoc, "A three-dimensional finite-strain rod model. Part II: Computational aspects," Computer Methods in Applied Mechanics and Engineering, vol. 58, no. 1, pp. 79–116, 1986.

[4] J. Simo and L. Vu-Quoc, "On the dynamics of flexible beams under large overall motions— the plane case: Part I," Journal of Applied Mechanics, vol. 4, no. 53, pp. 849–854, 1986.

[5] A. Neuenhofer and F. C. Filippou, "Geometrically nonlinear flexibility-based frame finite element," Journal of Structural Engineering, vol. 124, no. 6, pp. 704–711, 1998.

[6] M. Schulz and F. C. Filippou, "Non-linear spatial timoshenko beam element with curvature interpolation," International Journal for Numerical Methods in Engineering, vol. 50, no. 4, pp. 761–785, 2001.

[7] A. Cardona and M. Geradin, Flexible Multibody Dynamics: A Finite Element Approach, English. UK: John Wiley and Sons, 2001.

[8] D. Hodges, "Proper definition of curvature in nonlinear beam kinematics," American Institute of Aer vol. 22, no. 12, pp. 1825–1827, 1984.

[9] D. Luenberger and Y. Yu, Linear and Nonlinear Programming, English. New York,NY: Springer, 2008.

[10] K. Washizu, Variational Methods in Elasticity and Plasticity, English. Pergamon Press, 1975.

[11] J. Simo and T. Hughes, Computational Inelasticity, English. New York,NY: Springer, 1998.

[12] C. P. Andriotis, K. G. Papakonstantinou, and V. K. Koumousis, "Nonlinear programming hybrid beam-column element formulation for large-displacement elastic and inelastic analysis," Journal of Engineering Mechanics, vol. 144, no. 10, p. 04 018 096, 2018.

[13] M. Crisfield, "A fast incremental/iterative solution procedure that handles "snap-through"," Computers & Structures, vol. 13, no. 1–3, pp. 55–62, 1981.

[14] G. Cowper, "The shear coefficient in timoshenko's beam theory," Journal of Applied Mechanics, vol. 33, no. 2, pp. 335–340, 1966.

[15] J. Simo and R. Taylor, "A return mapping algorithm for plane stress elastoplasticity," International Journal for Numerical Methods in Engineering, vol. 22, no. 3, pp. 649–670, 1986.

[16] A. Papachristidis, M. Fragiadakis, and M. Papadrakakis, "A 3d fibre beam-column element with shear modelling for the inelastic analysis of steel structures," Computational Mechanic vol. 45, no. 6, pp. 553–572, 2010.

[17] A. Saritas and F. C. Filippou, "Frame element for metallic shear-yielding members under cyclic loading," Journal of Structural Engineering, vol. 135, no. 9, pp. 1115–1123, 2009.

[18] P. Ceresa, L. Petrini, R. Pinho, and R. Sousa, "A fibre flexure–shear model for seismic analysis of rc-framed structures," Earthquake Engineering & Structural Dynamics, vol. 38, no. 5, pp. 565–586, 2009.

[19] J. N. Gregori, P. M. Sosa, M. F. Prada, and F. C. Filippou, "A 3d numerical model for reinforced and prestressed concrete elements subjected to combined axial, bending, shear and torsion loading," Engineering Structures, vol. 29, no. 12, pp. 3404–3419, 2007.

[20] A. Kagermanov and P. Ceresa, "Fiber-section model with an exact shear strain profile for two-dimensional rc frame structures," Journal of Structural Engineering, vol. 143, no. 10, p. 04 017 132, 2017.

[21] J. C. Simo and T. J. Hughes, Computational inelasticity. Springer Science & Business Media, 2006, vol. 7.

[22] M. L. Wilkins, "Calculation of elastic-plastic flow," California Univ Livermore Radiation Lab, Tech. Rep., 1963.

[23] R. H. Dodds Jr, "Numerical techniques for plasticity computations in finite element analysis," Computers & Structures, vol. 26, no. 5, pp. 767–779, 1987.

[24] F. De Angelis and R. L. Taylor, "An efficient return mapping algorithm for elastoplasticity with exact closed form solution of the local constitutive problem," Engineering Computatio vol. 32, no. 8, 2015.

[25] J. Clausen, L. Damkilde, and L. Andersen, "Efficient return algorithms for associated plasticity with multiple yield planes," International Journal for Numerical Methods in Engineering, vol. 66, no. 6, pp. 1036–1059, 2006.

[26] O. Hopperstad and S Remseth, "A return mapping algorithm for a class of cyclic plasticity models," International Journal for Numerical Methods in Engineering, vol. 38, no. 4, pp. 549–564, 1995.

[27] W. M. Scherzinger, "A return mapping algorithm for isotropic and anisotropic plasticity models using a line search method," Computer Methods in Applied Mechanics and Engineerin vol. 317, pp. 526–553, 2017.

[28] A. R. Hartloper, A. de Castro e Sousa, and D. G. Lignos, "Constitutive modeling of structural steels: Nonlinear isotropic/kinematic hardening material model and its calibration," Journal of Structural Engineering, vol. 147, no. 4, p. 04 021 031, 2021.

[29] J. C. Simo and R. L. Taylor, "Consistent tangent operators for rate-independent elastoplasticity," Computer methods in applied mechanics and engineering, vol. 48, no. 1, pp. 101–118, 1985.

[30] M Ortiz and E. P. Popov, "Accuracy and stability of integration algorithms for elastoplastic constitutive relations," International journal for numerical methods in engineering, vol. 21, no. 9, pp. 1561–1576, 1985.

VITA

Vita may be provided by doctoral students only. The length of the vita is preferably one page. It may include the place of birth and should be written in third person. This vita is similar to the author biography found on book jackets.